International Journal of Extreme Manufacturing

3D printing critical materials for rechargeable batteries: from materials, design and optimization strategies to applications

OPEN ACCESS
IOP Publishing | IMMT
International Journal of Extreme Manufacturing
Int. J. Extrem. Manuf. **5** (2023) 042008 (31pp)
https://doi.org/10.1088/2631-7990/acf172

Topical Review

3D printing critical materials for rechargeable batteries: from materials, design and optimization strategies to applications

Yongbiao Mu[1,2,3,4], Youqi Chu[1,2,3,4], Lyuming Pan[1,2,3,4], Buke Wu[1,2,3], Lingfeng Zou[1,2,3], Jiafeng He[1,2,3], Meisheng Han[1,2,3], Tianshou Zhao[1,2,3,*] and Lin Zeng[1,2,3,*]

[1] Shenzhen Key Laboratory of Advanced Energy Storage, Southern University of Science and Technology, Shenzhen 518055, People's Republic of China
[2] SUSTech Energy Institute for Carbon Neutrality, Southern University of Science and Technology, Shenzhen 518055, People's Republic of China
[3] Department of Mechanical and Energy Engineering, Southern University of Science and Technology, Shenzhen 518055, People's Republic of China

E-mail: zhaots@sustech.edu.cn and zengl3@sustech.edu.cn

Received 6 March 2023, revised 26 May 2023
Accepted for publication 16 August 2023
Published 4 September 2023

Abstract

Three-dimensional (3D) printing, an additive manufacturing technique, is widely employed for the fabrication of various electrochemical energy storage devices (EESDs), such as batteries and supercapacitors, ranging from nanoscale to macroscale. This technique offers excellent manufacturing flexibility, geometric designability, cost-effectiveness, and eco-friendliness. Recent studies have focused on the utilization of 3D-printed critical materials for EESDs, which have demonstrated remarkable electrochemical performances, including high energy densities and rate capabilities, attributed to improved ion/electron transport abilities and fast kinetics. However, there is a lack of comprehensive reviews summarizing and discussing the recent advancements in the structural design and application of 3D-printed critical materials for EESDs, particularly rechargeable batteries. In this review, we primarily concentrate on the current progress in 3D printing (3DP) critical materials for emerging batteries. We commence by outlining the key characteristics of major 3DP methods employed for fabricating EESDs, encompassing design principles, materials selection, and optimization strategies. Subsequently, we summarize the recent advancements in 3D-printed critical materials (anode, cathode, electrolyte, separator, and current collector) for secondary batteries, including conventional Li-ion (LIBs), Na-ion (SIBs), K-ion (KIBs) batteries, as well as Li/Na/K/Zn metal batteries, Zn-air batteries, and Ni–Fe batteries. Within these sections, we discuss the 3DP precursor, design

* Authors to whom any correspondence should be addressed.
[4] These authors contributed equally to this work.

2631-7990/23/042008+31$33.00

principles of 3D structures, and working mechanisms of the electrodes. Finally, we address the major challenges and potential applications in the development of 3D-printed critical materials for rechargeable batteries.

Keywords: additive manufacturing, 3D printing, rechargeable batteries, electrochemical energy storage devices, lithium-ion battery

1. Introduction

Renewable fuels (such as, wind, solar, and hydroelectric power) are essential for the current settings of an ecologically friendly energy landscape due to the rising energy demands and the decrease in the consumption of fossil fuels [1, 2]. As examples of electrochemical energy storage devices (EESDs), numerous batteries and multiple-type super-capacitors reveal appreciable energy and power densities, great rate capabilities, and lengthy cycling lifetimes [3–5]. Due to the capacity of storing and supplying electric energy and the accessibility in varieties of forms, capacities, and power densities [6, 7], rechargeable batteries have received substantial attention and have been further researched. In order to enhance the electrochemical behaviors of batteries, lower their cos, and broaden their use, significant research has been made into developing new printable materials, electrolytes, battery architectures, and unique production technologies [8–10]. Nevertheless, electrochemically active substances could be coated onto two-dimensional (2D) current collectors during the normal battery production process, for example, the conventional planar electrodes of lithium-ion batteries (LIBs). The electrochemical performance could be negatively impacted by this strategy's potential to produce lengthy ions transport channels and small interfacial surface active areas [11]. Fabricating thicker electrodes, in particular, can considerably raise mass loadings of material while maintaining rapid ions diffusion in order to attain high energy densities and areal capacities. Moreover, integrated batteries (containing anode, cathode, and electrolyte) are needed, which current battery construction processes cannot achieve [12, 13]. Furthermore, creating 3D porous structure with enlarged surface areas can accelerate electrode reaction rate and ion transfer, meanwhile, efficient use of limited space in compact cell systems can result in shorter ion diffusion paths, lower interface resistance and charge transfer resistance. As a result, creating different kinds of electrodes with 3D structures combined with different aperture sizes using a controlled and producible technique remains a substantial difficulty [14, 15].

Manufacturing method is critical for realizing perfect EESD shapes and better electrochemical performance, and the demand for sustainable and innovative manufacturing is growing [16–18]. Additive manufacturing (AM), an industrial manufacturing process, creates 3D things by layering active materials directly from pre-designed drawings and procedures by computer [19–22]. This technique, often known as 3D printing (3DP), is a unique kind of fabrication methods that allows for developing complex frameworks under a cheaper cost than traditional processing techniques [16, 23, 24]. When compared to conventional methods for batteries, 3DP possesses lots of notable advantages: firstly, enabling any desired shapes to construct complex 3D architectures can be achieved; secondly, the shapes and thickness of the electrodes can be specifically regulated to acquire breath-taking areal and volumetric densities; thirdly, solid-state electrolytes (SSEs) with high structural stability and safe operations are synthesized via directly printing polymer or composite printing inks; in addition, lower manufacturing costs and environmental friendliness make its application more widespread and universal [25]. Moreover, 3DP can drastically reduce unnecessary material waste and may potentially improve efficiency because of the less sophisticated fabrication processes. On the whole, 3DP opens new doors for 3D-structured battery prototyping with distinctive architectures and outstanding performance.

Considerable research efforts have been dedicated to multiple reviews summarizing and discussing 3D-printed EESDs. However, limited attention has been given to the discussion of 3D-printed anodes, separators/cathodes, electrolytes, and 3D hosts, specifically focusing on ink formulation, electrode structures, and optimization strategies for 3D electrode structures. Capitalizing on the aforementioned advantages, we present a comprehensive review of recent progress in critical materials and novel designs for 3D-printed rechargeable secondary batteries (scheme 1). The review is organized into three main sections. Firstly, we provide an overview of various types of 3DP techniques employed for EESDs from 2013 to 2022, encompassing methods, printable materials, and types of electrode structures (figure 1(a)). This section summarizes a wide range of 3DP technologies, with particular emphasis on their applications in the field of new energy. The discussion includes polymer matrices used for printing, functionalized materials, and common characteristic structures. Secondly, we delve into several 3D-printed key materials in rechargeable batteries, including cathodes, anodes, electrolytes/separators, and current collectors. We extensively explore the details of 3DP technology applied to electrode materials, structural design, and reaction mechanisms. Finally, we conclude the review by highlighting the challenges and future prospects of 3DP in the realm of rechargeable secondary batteries.

2. 3DP technology

3DP, also referred to as rapid manufacturing, involves the creation of digital model files based on the 'discrete-stacking' theory. It operates by printing materials, such as powdered

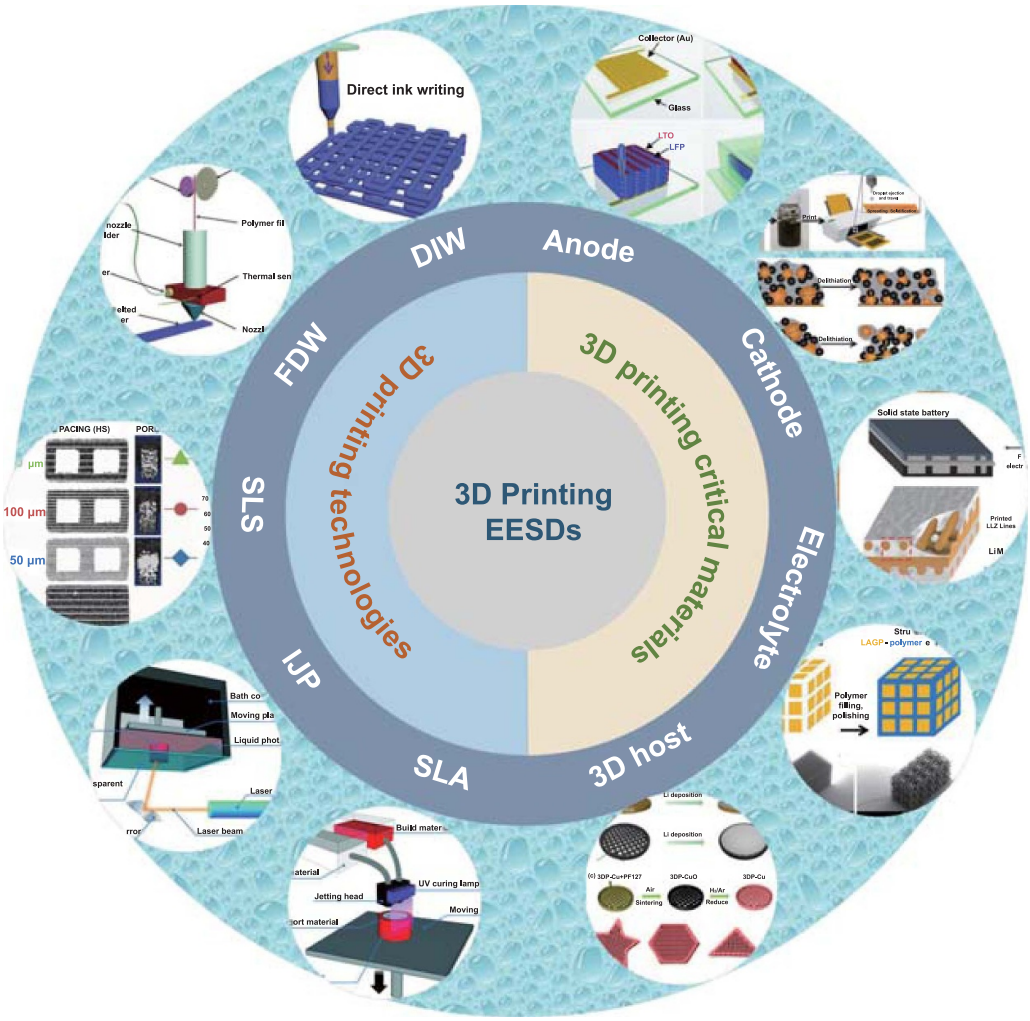

Scheme 1. Diagram of this review of 3D-printed rechargeable secondary-batteries: 3DP techniques and critical components in EESDs. Reprinted from [26], Copyright (2017), with permission from Elsevier. Reproduced from [27] with permission from the Royal Society of Chemistry. [28] John Wiley & Sons. [© 2021 Wiley-VCH GmbH]. [29] John Wiley & Sons. [© 2018 WILEY-VCH Verlag GmbH & Co. KGaA, Weinheim]. [30] John Wiley & Sons. [Copyright © 2013 WILEY-VCH Verlag GmbH & Co. KGaA, Weinheim]. Reproduced from [31] with permission from the Royal Society of Chemistry. [32] John Wiley & Sons. [© 2019 WILEY-VCH Verlag GmbH & Co. KGaA, Weinheim].

metal or plastic, layer by layer under computer control to produce a three-dimensional (3D) object. Generally, 3DP technologies can be categorized into the following types based on their method and operating principle: (1) material extrusion techniques (e.g. fused deposition modeling (FDM), fused filament fabrication (FFF), direct ink writing (DIW)); (2) powder bed fusion methods (e.g. selective laser melting (SLM), selective laser sintering (SLS), electron-beam melting, direct metal laser sintering); (3) light polymerization processes (e.g. stereolithography (SLA), digital light processing (DLP), laser cladding deposition); (4) material jetting approaches (e.g. inkjet printing (IJP)); (5) binder jetting methods; and (6) sheet lamination techniques (e.g. laminated object manufacturing (LOM)).

Some reliable reviews [3, 33] have comprehensively summarized the features of various 3DP technologies. Moreover, the selection of appropriate 3DP materials is crucial as it forms the foundation for the widespread application of 3D technology. Different 3DP materials exhibit distinct characteristics, but the mechanical properties, processing properties, heat resistance, corrosion resistance, and chemical stability of these materials significantly impact the progress of 3DP technologies. Currently, there are several types of 3D printable materials available, including thermoplastics, light-cured resins, ceramics, rubbers, metals, and other novel materials. However, not all 3DP materials and technologies are suitable for fabricating EESDs, particularly in the field of rechargeable batteries. Furthermore, an important challenge in 3DP lies in the preparation of ink, which directly influences the macroscale accuracy, micro-porosity, and electrochemical properties of printed electrodes. The ink formulation must satisfy specific requirements, such as appropriate viscosity, high shear and compression yield stress, controllable viscoelastic rheological parameters, high solid content, and excellent electrical conductivity. Achieving these characteristics in the ink is essential for successful 3DP of electrodes.

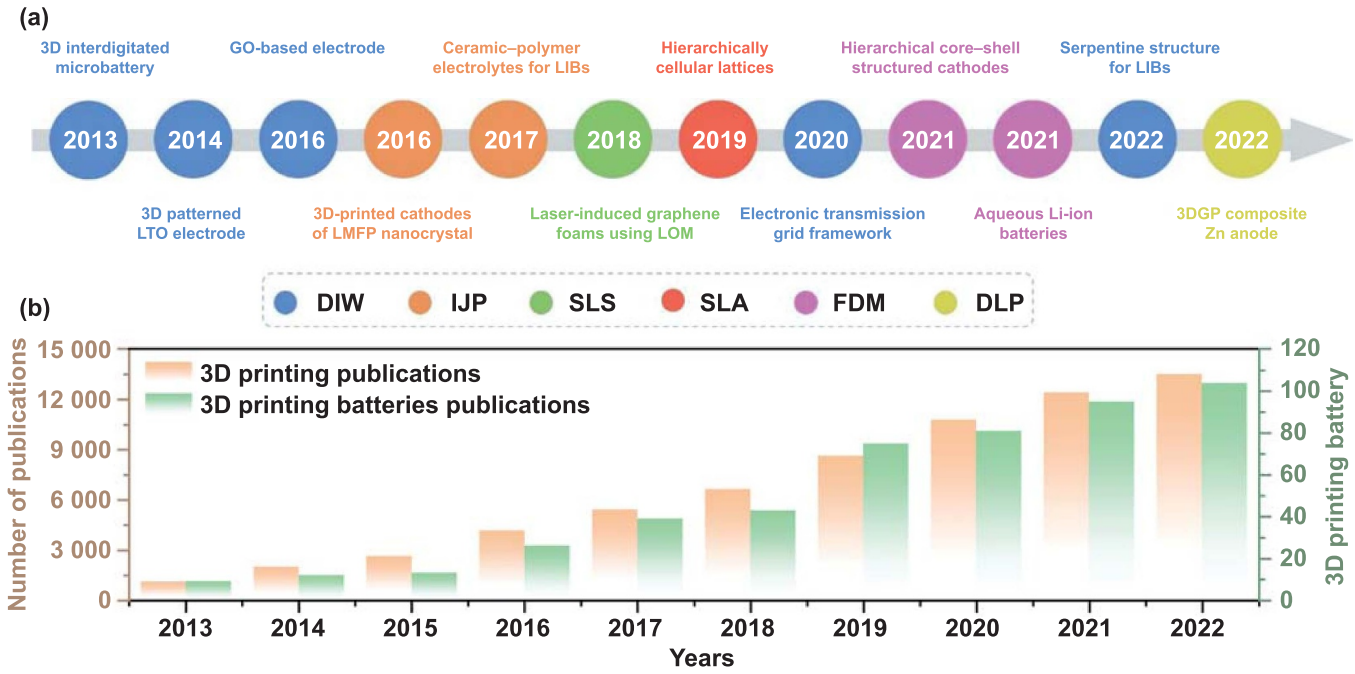

Figure 1. The development of 3D printing technologies in secondary batteries. (a) A timeline of 3D printing technologies, structures, and materials for EESDs, and (b) the publications and trends on 3D printing and 3D-printed batteries from 2013 to 2022 (data from web of science).

Different 3DP techniques also have notable drawbacks. For instance, the FDM method involves a complex material preparation process and high organic binder content, resulting in electrodes with low specific energy and conductivity. DIW suffers from low solid content, high rheological properties, poor process stability, and challenges in forming thicker electrode structures. IJP requires well-distributed particle sizes, good fluidity, and stable chemical properties at high temperatures. Additionally, IJP technology has limitations in terms of printing height and the inability to produce internal porous structures. Therefore, our focus is on popular 3DP techniques and critical materials used in rechargeable devices, allowing for a comprehensive understanding of the characteristics and advancements of various 3D-printed components in EESDs. Table 1 provides a summary of different 3DP technologies and printing materials. As an advanced material processing technology, 3DP offers numerous advantages in industrial manufacturing and has reached a high level of technological maturity. In the academic realm, researchers have conducted extensive investigations on 3DP, including the exploration of printing materials from technical sources and practical applications, particularly in the field of EESDs.

Binder jetting printing (figure 2(a)), in conjunction with powder-bed and powder supply, enables the fabrication of intricate structures [34]. During the production process, a leveling roller uniformly distributes a micron layer of powder from the powder supply onto the bed. Subsequently, the printer head's nozzle inkjets the binder onto the bed powder, causing the powder to adhere to the adjacent layer. The powder platform then moves downward along the *Z*-axis, gradually constructing the desired structures layer by layer.

Vat photopolymerization (figure 2(b)) utilizes a photopolymer resin that undergoes selective curing in a vat through active polymerization in the presence of a light source, such as UV light. Specifically, SLA is a type of photopolymerization printing technology that employs an ultraviolet (UV) laser beam directed onto a vat filled with UV-curable photopolymer resin. The resin located at the vat surface, where the UV laser beam strikes, undergoes photochemical curing and solidification due to the UV light. Motor-controlled mirrors are used to generate a pre-programmed single layer. The build platform then lowers by a predetermined layer height, and a moving blade applies a fresh coating of resin on top of the resin tank. This process is repeated until each layer is cured based on the model, resulting in the completion of the 3D object. Sheet lamination (figure 2(c)) involves the assembly of cut sheets of materials such as polymers, metals, or paper in a layer-by-layer fashion to create the desired object. A mirror moves along the *X* and *Y* axes to direct the light source towards the sheet, while the build platform moves along the *Z* axis to receive the stack of sheets with the cut region. Each layer's corresponding sheet is cut using a laser or another cutting instrument to match a previously formed shape. Finally, the excess sheets along the contour of the object are removed to reveal the finished product.

Powder bed fusion (figure 2(d)) utilizes a powder bed and a powder supply to selectively melt and fuse powder particles, enabling the fabrication of complex structures. One of the

Table 1. Comparisons of 3DP technologies for various rechargeable batteries.

Categories	Methods	Main materials	Advantages	Limitations	Main applications	References
Materials extrusion	DIW	Plastics; Ceramic; Metal; Composites	Low cost; simply fabrication process; material flexibility; easy operation	Inferior mechanical Properties; high requirement of ink	LIBs; SIBs; redox flow batteries	[35–40]
Materials extrusion	FDM	Thermoplastics: ABS; PLA; PC	Affordable cost; high speed; Simplicity	Weak mechanical Properties; limited active materials	LIBs; SIBs	[21, 35, 41]
Powder bed fusion	SLS	Polymer based; powder	High resolution; no support; structure needed	Exorbitant; Limited mechanical properties of object	LIBs; Al-air batteries; RFBs	[22, 35, 42, 43]
Powder bed fusion	SLM	Metal powders; Metal alloy powders	High utilization; direct production of metal parts	High cost; slow printing speed	LIBs	[17, 44, 45]
Vat photopolymerization	SLA	Photopolymers	High efficiency; high resolution; high quality	Need photosensitive additives; single material	LIBs; supercapacitor	[44–47]
Materials jetting	IJP	Metal Conductive polymers Ceramics Gel	High printing precision; no support structure needed	Low surface quality Sluggish printing speed Poor long-term durability	LIBs Zn-air batteries RFBs	[17, 22, 48–50]
Binder jetting	Binder jetting	Any material in particulate form Metal powder Ceramics powder	Low temperature; no support materials	Limited mechanical properties Low surface quality	LIBs RFBs	[17, 22, 51, 52]
Sheet lamination	LOM	Laminated sheets Paper metal Plastic	Fast forming; affordable cost; large size samples	Weak mechanical properties Design limitations	LIBs	[17, 53]

techniques employed in powder bed fusion is SLS, which involves the fusion of a layer of powder particles along a defined path using a high-energy source, such as a laser beam. After the first layer has solidified, the build platform is lowered to accommodate the next layer of powder particles. This process is repeated until all the layers have been fused, and any remaining unfused powder is removed, resulting in the desired 3D printed structure.

Directed energy deposition (figure 2(e)) utilizes a precisely focused power source to simultaneously melt the substrate and the material being added to the substrate melt pool. The build platform moves along the *X, Y*, and *Z* axes, while the print head remains stationary. The print head creates a path of solidified material, and as these paths intersect, they form the printed layer. By overlapping these paths layer by layer, a complex 3D structure is formed.

Material extrusion (figure 2(f)) involves layering molten or semi-molten polymer, paste, or polymer solution through a printing head equipped with a nozzle or aperture. After depositing the first layer, the print head or platform moves along the *Z*-axis to enable the deposition of subsequent layers. DIW is a form of material extrusion that begins with the development of a viscoelastic ink with specific rheology. The desired 3D structure is then constructed by extruding continuous filaments placed on a building platform through a nozzle at a controlled pressure. For DIW, it is crucial to develop an ink with appropriate viscosity and elastic behavior, particularly ensuring suitable yield stress behavior for successful printing. Another common extrusion-based printing technology, FDM, involves layering thermoplastic filaments that have been heated to a semi-molten state at the nozzle tip before extrusion. The extruded material quickly solidifies on the build platform at a lower temperature, forming a solid layer that is subsequently built upon to create the final 3D object, guided by CAM or CAD software.

In the material jetting technique (figure 2(g)), the material and binder are combined at the printing head and dispersed into tiny droplets, which are selectively deposited through an aperture onto the platform. The applied material can be cured either by a light source or by the surrounding atmosphere, depending on the specific material being used.

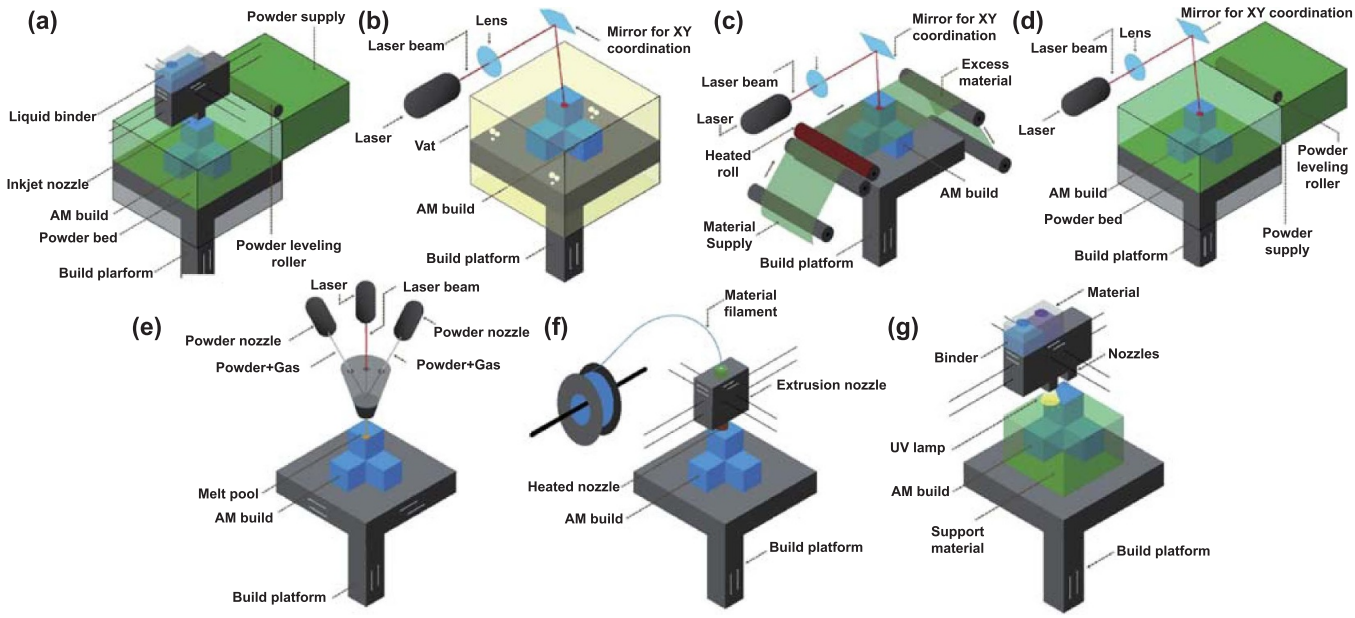

Figure 2. 3D printing technologies categories: (a) binder jetting, (b) vat photo-polymerization, (c) sheet lamination, (d) powder bed fusion, (e) directed energy deposition, (f) material extrusion and (g) material jetting. Reprinted from [34], Copyright (2020), with permission from Elsevier.

3. Printable battery modules and structures

3DP technology has demonstrated significant potential in the fabrication of EESDs. Analysis of publications and the utilization of 3DP technologies in batteries using the 'Web of Science' database reveals the increasing prevalence of 3DP technology, particularly in emerging battery types (figure 1(b)). Rechargeable secondary batteries, including Ni–Cd, lead-acid, Ni-metal hydride, LIBs, and flow batteries, dominate the battery market due to their ability to undergo repeated charge and discharge cycles [54–56]. Although active electrodes based on intercalation/deintercalation mechanisms exhibit excellent cycling performance, their energy and power densities are limited by the limited number of intercalated ions and slow reaction kinetics [57, 58].

Conventional 2D electrodes often rely on strategies such as increasing electrode thickness and loading of active materials to enhance specific capacitance and energy density. However, thick electrodes suffer from uneven pore distribution and long ion transport pathways, resulting in sluggish ion and electron transport and a decrease in power density and rate performance. In contrast, 3DP technology, a layer-by-layer AM technique with customizable structures, enables the production of intricate spatial frameworks with superior structural design and integration. The resulting electrodes facilitate electrolyte permeation and ion diffusion, addressing the limitations associated with traditional 2D electrodes.

Several distinctive 3DP structures have been documented, including grid structures, interdigitated structures, serpentine structures, fibrous structures, hierarchical octet-truss structure, and others, as illustrated in figure 3 [59, 60]. The stacked 3D-printed grid structure is formed by stacking multiple grid layers, each composed of two perpendicular parallel lines, along the *Z* axis (figure 3(a)) [61]. This structure features layered and ordered pores, resulting in a high specific surface area and promoting uniform electron distribution on the electrode surface. Consequently, it reduces local current density during charge and discharge processes, leading to improved active material utilization. Furthermore, the porous nature of this structure helps alleviate mechanical stress within the electrode, enhancing its mechanical properties. Additionally, the 3D-stacked electrode structure facilitates efficient electrolyte transport and penetration, ultimately enhancing power performance.

The interdigitated structure electrode consists of a 3D-printed framework with cathode and anode electrodes interconnected in an interlaced 'finger' arrangement (figure 3(b)) [15]. This design enhances the contact area between the electrodes and reduces ion transfer distance, thus reducing resistance in integrated cells. Complex interdigital electrodes can only be produced using 3DP techniques, such as DIW and FDM. Serpentine structure electrodes, created by 3DP serpentine patterns, exhibit reversible stretchability at the component level, showcasing their potential for stretchable energy storage devices in wearable and flexible electronics (figure 3(c)) [62]. Fibrous structures (figure 3(d)) obtained through 3DP exhibit flexibility, breathability, and meet the requirements for wearable energy storage devices [63]. These fibrous electrodes demonstrate excellent flexibility, electrochemical performance, and sufficient porosity for air exchange and stretching capability. The hierarchical octet-truss structure, with its stable triangular architecture, exhibits exceptional stiffness and strength (figure 3(e)) [64]. As a unique hierarchically porous structure, it offers significant advantages in the application of energy storage devices. Thus, various complex spatial structures are fabricated using 3DP technologies, providing significant benefits for energy storage device applications.

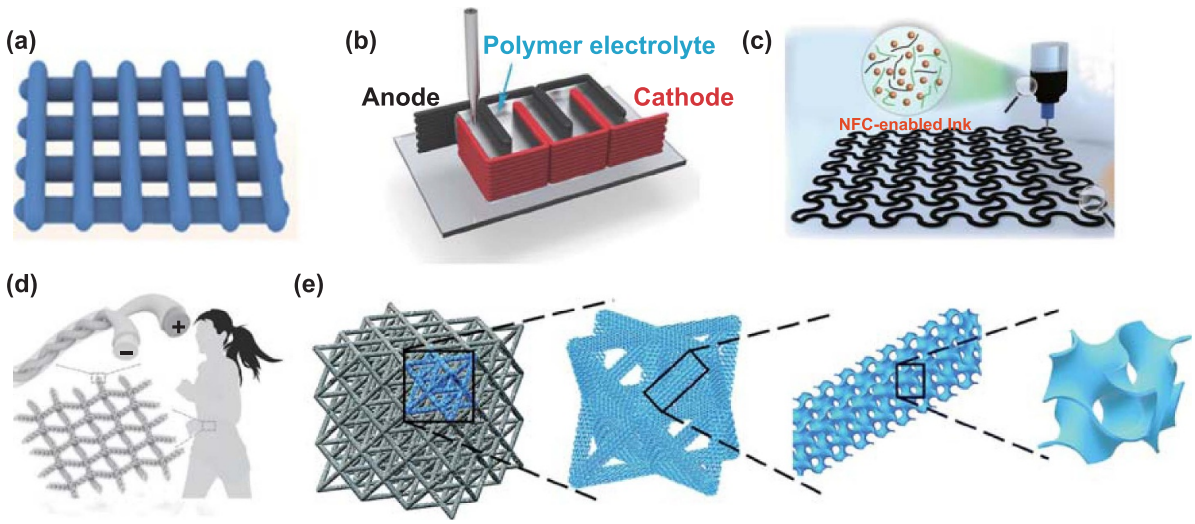

Figure 3. Typical 3D printing architectures of electrodes. Schematic of (a) the grid structure. Reprinted from [61], Copyright (2023), with permission from Elsevier. (b) The interdigitated structure. [15] John Wiley & Sons. [© 2016 WILEY-VCH Verlag GmbH & Co. KGaA, Weinheim]. (c) The serpentine structures. Reprinted from [62], Copyright (2022), with permission from Elsevier. (d) The fibrous structures. [63] John Wiley & Sons. [© 2017 WILEY-VCH Verlag GmbH & Co. KGaA, Weinheim] and (e) the hierarchical octet-truss structure. Reproduced from [64] with permission from the Royal Society of Chemistry.

Designing and fabricating 3D architectures for critical components, including electrodes (cathode and anode), separator/electrolyte, and current collector, have emerged as effective approaches to optimize structures and improve battery performance [65, 66]. The utilization of 3DP approaches in rechargeable batteries has been demonstrated to enhance the basic capabilities of these critical components [67], which in turn determine the overall properties of the battery, such as energy densities, power densities, cycle lifespan, and safety [68, 69]. Thus, in this section, we focus on the architectural aspects of currently available printed battery modules [70]. These individual battery modules require qualities such as mechanical robustness, excellent electrical and ionic conductivity [16, 71], and the selection and utilization of appropriate 3DP procedures and materials are crucial for achieving these goals in energy storage and conversion systems, further driving advancements in other energy storage systems [72].

In 2013, Lewis *et al* demonstrated the printing of micro-LIBs with an interdigitated design using DIW, which included the commonly used anode and cathode of LIBs [73, 74]. The 3D interdigitated design and DIW process provided an advantageous approach for the stacking and placement of battery components [15]. Since then, researchers have continuously developed novel electrode structures and materials, assembling them through various 3DP processes. Prior to 2013, some attempts were made to produce 3D-architected electrodes or batteries using IJP, but they were mostly limited to 2D frameworks with restricted information and functionalities [75, 76]. Therefore, this review focuses on the application of 3DP technologies in rechargeable batteries, primarily including LIBs, sodium-ion batteries (SIBs), solid-state Li batteries, Li-air batteries, Li–S batteries, and zinc-ion batteries (ZIBs) [77] (figure 4). We emphasize and discuss design principles, material selection, structural optimization, and electrochemical performance mechanisms in different electrochemical systems.

4. 3D-printed cathode materials

The preparation of inks is crucial for 3D-printed critical materials used in rechargeable batteries, involving the selection of raw materials and the composition ratio of the ink. Various types of raw materials are used for different battery components, such as cathode ink, anode ink, electrolyte/separator ink, and more. The proportion of ink components varies depending on the specific battery type. Among these components, enhancing the performance of the cathode material plays a significant role in improving the overall battery performance. 3DP technology can be employed to design cathode electrode materials for batteries, enabling control over the morphology of the printed cathode materials at both macro and micro scales. This control facilitates the transformation from a 2D electrode to a 3D electrode, enhancing the surface activity of the electrode and facilitating ion and electron transport within the electrode. Additionally, the controllable thickness of the cathode electrode material allows for adjustment of the active substance mass, ultimately achieving high energy density and high power density in lithium batteries [15, 78].

In the field of LIBs, several major cathode materials have been successfully printed, including $LiFePO_4$ [79], $LiMn_{1-x}Fe_xPO_4$, $LiCoO_2$ [80], $LiMn_2O_4$, and $LiNi_{0.8}Co_{0.15}Al_{0.05}O_2$ (NCA). Among them, $LiFePO_4$ has seen the most significant development and has been printed using various processes such as DIW, FDM, and IJP. To achieve high aspect ratios in printing electrode structures, it is essential to carefully tune the composition and rheology of inks. This ensures reliable flow through fine deposition nozzles, promotes adhesion between printing features, and

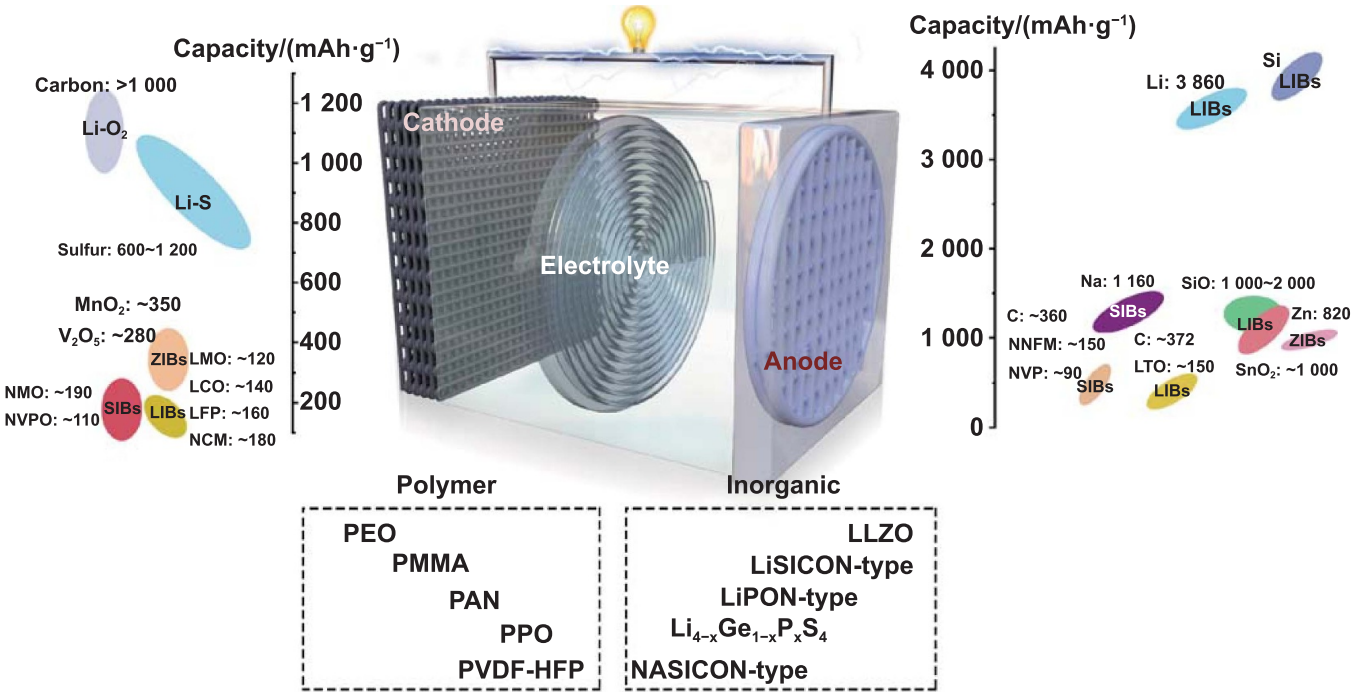

Figure 4. Schematic diagram of the critical materials and the lists of printable components including cathodes, anodes, and electrolytes for advanced rechargeable batteries.

provides the necessary structural integrity to withstand drying and sintering without delamination or deformation.

Lewis *et al* employed a straightforward 3DP approach by suspending $Li_4Ti_5O_{12}$ and $LiFePO_4$ nanoparticles in a solution containing deionized water, ethylene glycol, glycerin, and cellulose-based adhesives [30]. Multiple steps, including particle dispersion, centrifugation, and homogenization, were used to precisely generate filamentary functional inks on surfaces with varying densities from 100 $s{\cdot}m^{-2}$ to 1 $s{\cdot}m^{-2}$. They constructed a 3D staggered microcell structure (3D-IMA) composed of $Li_4Ti_5O_{12}$ (anode) and $LiFePO_4$ (cathode) using 3DP technology (figures 5(a)–(e)). These active materials exhibited modest volumetric expansion, reducing the need for electrode compliance to accommodate strain during charge/discharge operations. Printing thin LFP cathodes and LTO anodes enabled the realization of high area energy/power densities. The researchers demonstrated potential applications in self-powered biomedical and microelectronics devices by printing interdigitated electrodes, packing them, and electrochemically characterizing 3D Li-ion microbatteries.

Hu *et al* proposed a 3DP method and manufactured 3D LIBs using $C@LiMn_{1-x}Fe_xPO_4$ cathode [81]. Compared to conventional coated electrodes, the printed 3D LIBs exhibited ultra-high rate capabilities and capacities. Furthermore, using the pseudo-2D hidden Markov model (referred to as P2DHMM) and the simplified LIB model, the researchers found that electrolyte diffusion significantly influences the rate performance, including factors such as the solution's intrinsic diffusion coefficient, efficiency porosity, and electrode thickness. The printed battery achieved a capacity of 108.45 $mAh{\cdot}g^{-1}$ at 100 C, demonstrating the LMFP LIBs' superior rate capability (figure 5(f)). These results hold universal significance for future battery design, as they highlight the importance of regulating electrode thickness and porosity to achieve improved rates and capacities.

In addition, a low-cost cathode for LIBs has been produced, for instance, DIW had produced $Na_3V_2(PO_4)_3$ with a grid structure, and FDM had produced $NaMnO_2$ with a cylindrical shape [75]. Ding *et al* printed 3D porous skeletons for salt storage using GO-contained ink with special ratio and a freeze-drying method. Further demonstrating the wide applicability of GO-based inks in the construction of a variety of well-designed and structurally complex frames, four types of frames were printed, such as staggered grids, square coils, mosquito coils and circular arrays. Plenty of microholes and interconnected 3D networks were present in the as-obtained skeletons [82] (figure 6(a)). Surprisingly, the filaments were porous in a hierarchical manner and were cross-linked by a spate of flexible nanosheets (figures 6(b) and (c)). Scanning electron microscope (SEM) (figure 6(d)) revealed that the NVP particles were evenly distributed throughout the skeletons. The adjustable NVP-GO inks were used to print a variety of skeletons (for instances, triangle, square, circle) that could withstand the quick passage of sodium ions and electrons (figure 6(e)). Wei *et al* reported the design, fabrication, and electrochemical performance of fully 3D printed LIBs of LFP or LTO (figure 6(f)) [83]. The active electrode particles with good dispersion have small volume change and excellent thermal stability, and are mixed with conductive carbon to construct a permeable network. Fully 3D-printed LIBs eliminates the need for drying, electrolyte filling, calendering, clamping, and heat sealing processes associated with traditional LIB manufacturing, and delivered an areal capacity

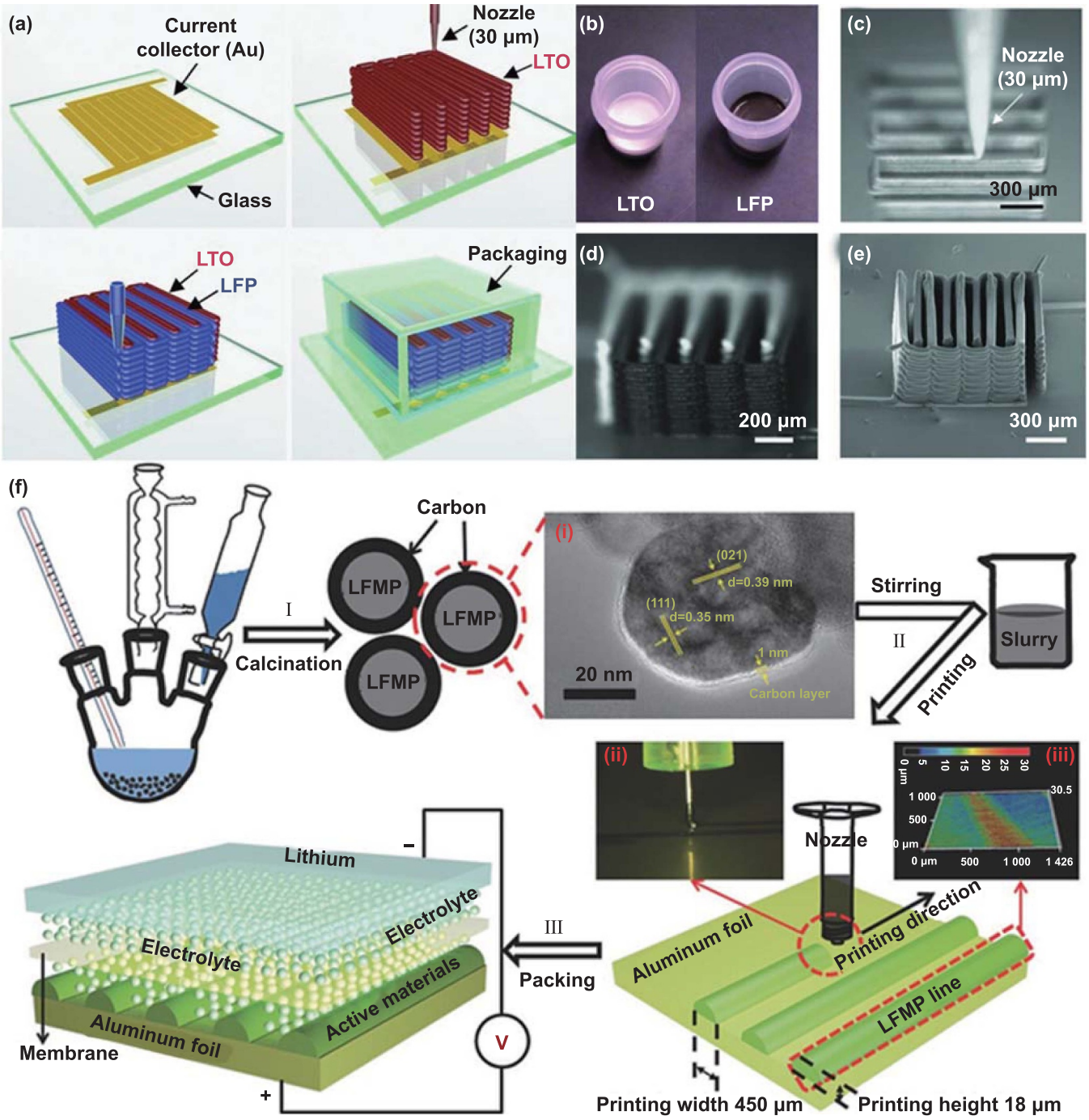

Figure 5. 3D printing of lithium-ion battery cathode materials. (a) Diagram of fabricating 3D LTO and LFP composite cathode. (b)–(e) Digital and SEM images, half-cell voltage of electrodes, and areal capacity of LTO-LFP electrode. [30] John Wiley & Sons. [Copyright © 2013 WILEY-VCH Verlag GmbH & Co. KGaA, Weinheim]. (f) Schematic of batteries fabrications with the 3DP electrode. [81] John Wiley & Sons. [© 2016 WILEY-VCH Verlag GmbH & Co. KGaA, Weinheim].

of 4.45 $mAh{\cdot}cm^{-2}$ at 0.14 $mA{\cdot}cm^{-2}$, which is equivalent to 17.3 $Ah{\cdot}l^{-1}$. Nickel-based (Ni–Zn, Ni–Fe) batteries are emerging as one of the new-type rechargeable batteries. Kong *et al*'s group [55] reported the 3D-printed quasi-solid-state Ni–Fe batteries (NFB) devices through layer-by-layer stacking 3DP technology. In this design, 1D carbon nantubes and 2D rGO sheets ink was employed to fabricate the free-standing matrix, and then ultrathin $Ni(OH)_2$ nanosheets and holey α-Fe_2O_3 nanorod arrays were prepared by solution method and hydrothermal method, respectively. Homogeneous GO-carbon nanotube (CNT) ink plays an important part in printing 3D self-support matrix. As a result, the Ni–Fe battery demonstrated superior cycling lifespan of 10 000 cycles with 91.3% capacity retentions and significant energy density of 28.1 $mWh{\cdot}cm^{-3}$ at a power of 10.6 $mW{\cdot}cm^{-3}$.

In recent years, the limited capacity of cathodes has been a major obstacle to achieving higher energy density in LIBs, hindering their development. To address this issue,

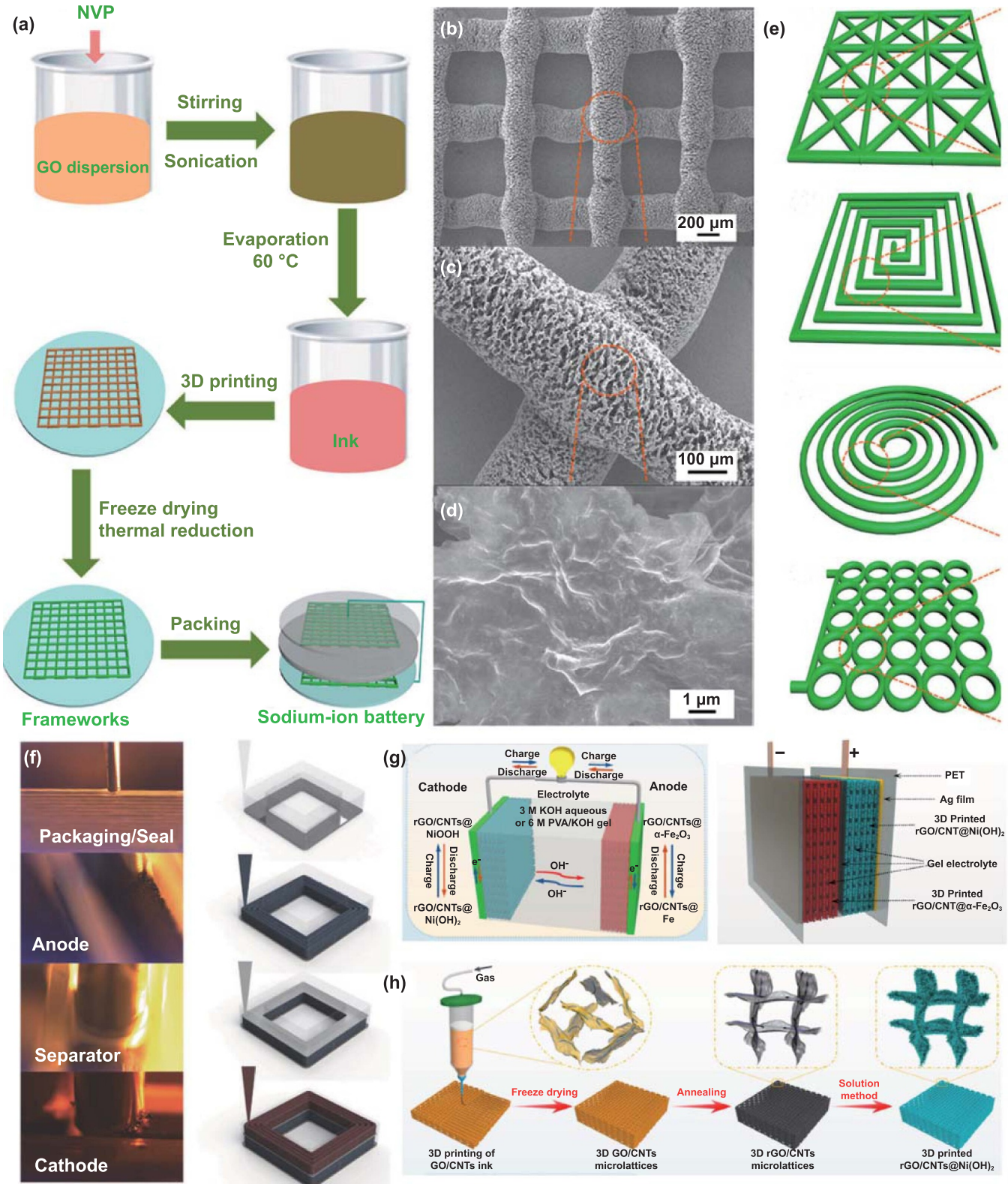

Figure 6. 3D-printed critical materials for SIBs, LIBs, and Ni–Fe battery. (a) Diagram of 3D-printing porous skeletons, (b)–(d) the corresponding SEM images of printed samples under different magnifications. (e) Schematics of different types of 3D-printed frameworks including triangle, square, and circle. Reprinted with permission from [82] Copyright (2017) American Chemical Society. (f) Images and schematics of direct writing inks of four components in LIBs. [83] John Wiley & Sons. [© 2018 WILEY-VCH Verlag GmbH & Co. KGaA, Weinheim]. (g) Working principle and electrochemical reaction mechanisms of the 3D-printed Ni–Fe battery, and (h) schematic illustration of fabrication of 3D-printed rGO/CNTs@$Ni(OH)_2$ cathode and 3D-printed rGO/CNTs@α-Fe_2O_3 anode. Reprinted with permission from [55] Copyright (2022) American Chemical Society.

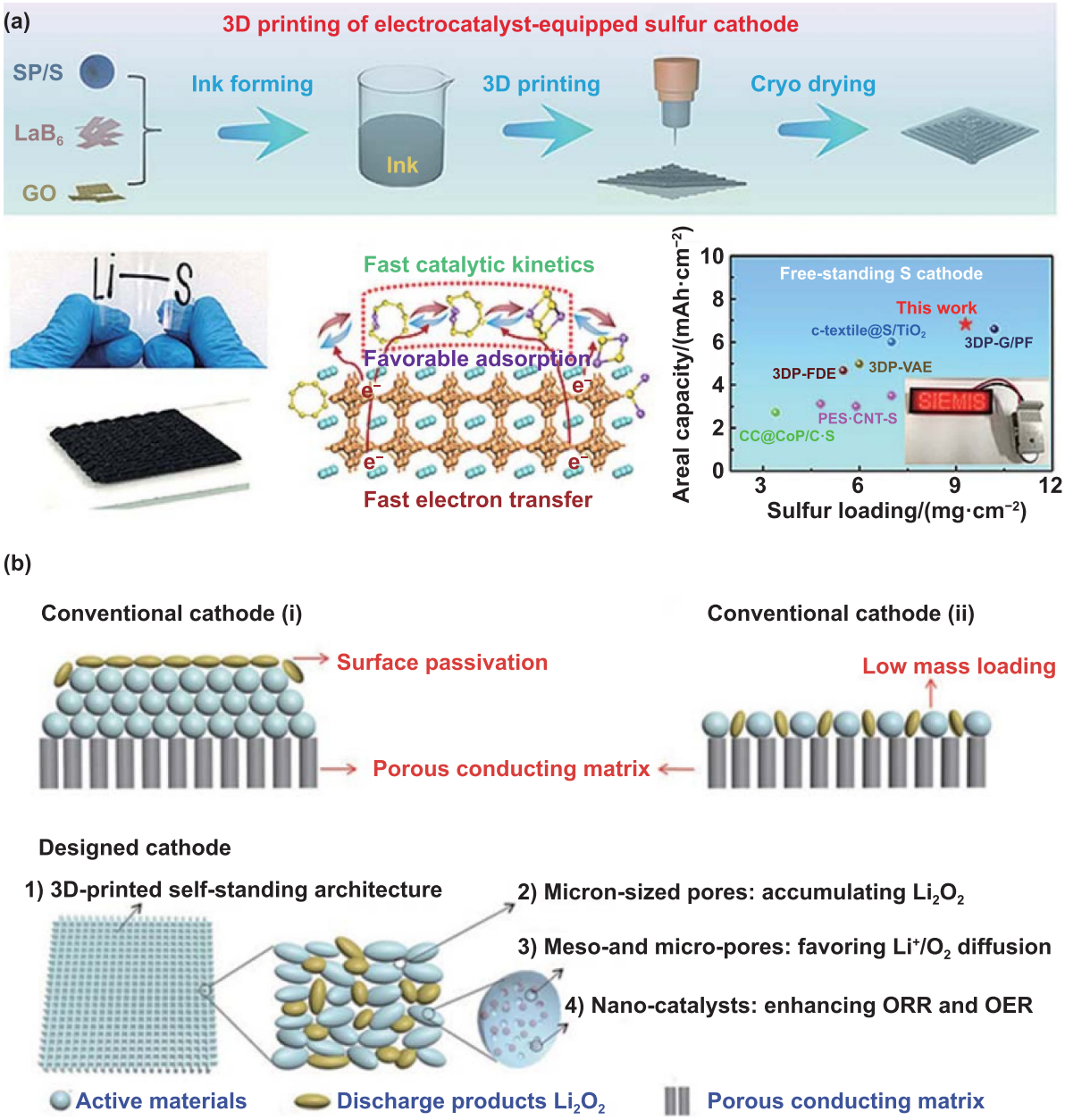

Figure 7. The applications of 3D printing technology in Li–S battery and Li-air battery. (a) Diagram of the 3D-printed 3D sulfur (S) cathode, optical picture, performance and analysis. Reprinted from [84], Copyright (2020), with permission from Elsevier. (b) The comparison of catalyst in Li-air system with 2D or 3D framework. [85] John Wiley & Sons. [© 2018 WILEY-VCH Verlag GmbH & Co. KGaA, Weinheim].

the use of 3DP technology to fabricate cathode materials with high theoretical mass specific capacity has emerged. For example, 3DP has been employed to print sulfur (S) cathodes for Li–S battery systems and catalysts for Li-air systems [74]. Cai *et al* developed a separate 3DP-LaB6/SP@S electrode using an extrusion-based 3D printer, involving three key steps: ink formulation, 3DP, and freeze drying [84] (figure 7(a)). The resulting cathode exhibited a densely packed structure with hierarchical microholes and continuous multichannels, facilitating unrestricted pathways for electrons and ions and effectively accommodating volume expansion over long-term cycling.

Furthermore, Lyu *et al* utilized 3DP technology to create a freestanding catalytic scaffold with abundant porous structures by employing cobalt-containing metal-organic framework (Co-MOF) ink derived from 2-methylimidazole and cobalt nitrate solution. The scaffold was carefully thermally treated using an extrusion-based 3D printer (figure 7(b)) [85]. The hierarchical frameworks comprised Co-MOF-derived carbon particles, which generated micrometer-sized openings and various-sized pores within the sheets. This resulted in a highly conductive, mechanically stable, and crack-free carbon structure that served as an excellent conducting matrix. By converting the permeable matrix into a self-standing catalyst

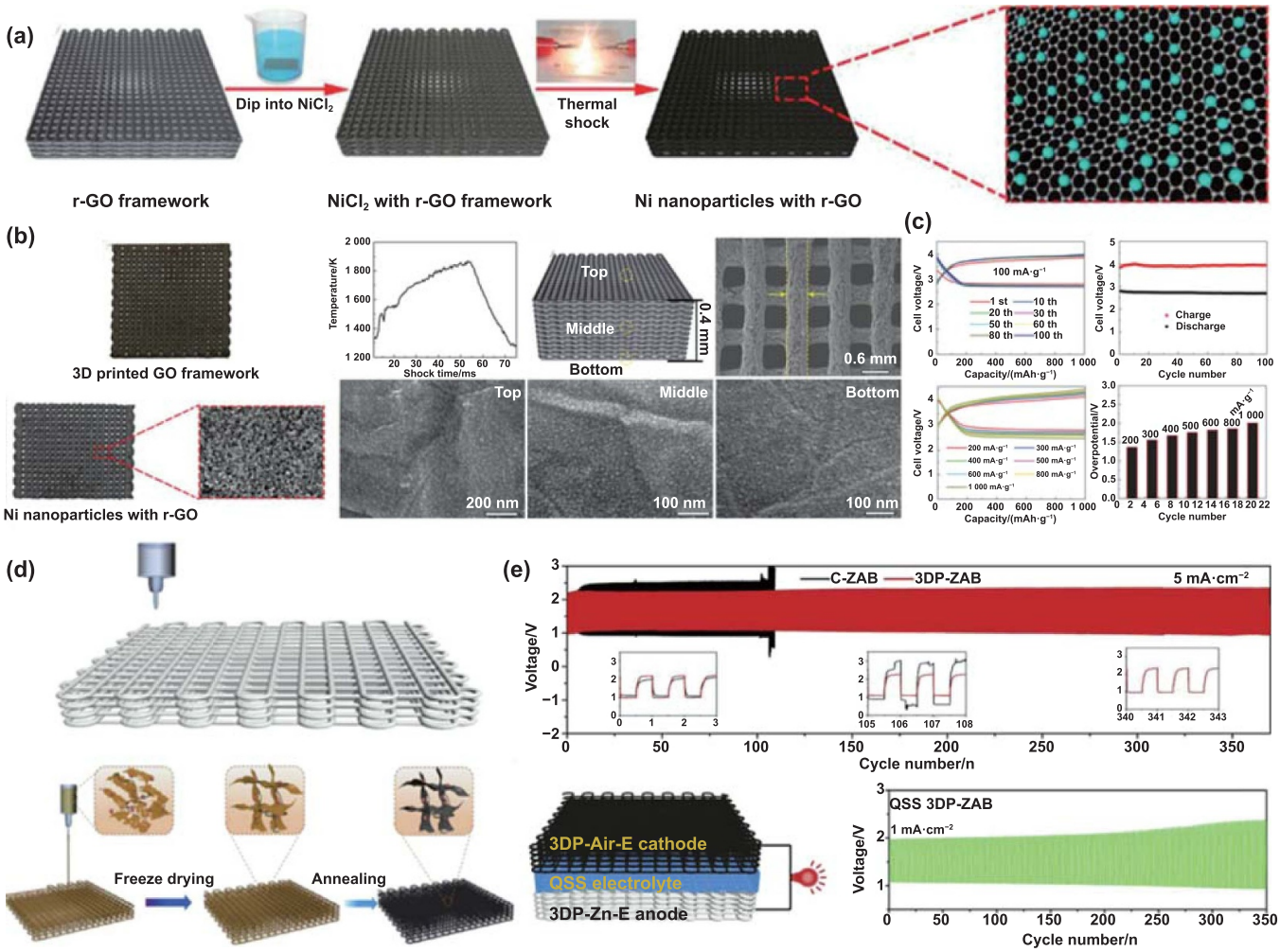

Figure 8. The applications of 3D printing technology in Li-CO_2 battery and Zn-air battery. (a) Diagram of fabricating r-GO framework by 3DP. (b) SEM, TEM and optical images of the GO, Ni/r-GO frameworks, (c) electrochemical properties. [86] John Wiley & Sons. [© 2018 WILEY-VCH Verlag GmbH & Co. KGaA, Weinheim]. (d) Schematics of 3D-printed anode and cathode in Zn-air battery and (e) electrochemical properties. Reprinted from [87], Copyright (2020), with permission from Elsevier.

design, the specific energy was significantly increased, leading to a competitive energy density.

In addition to the commonly studied Li–S and Li–O_2 cathodes, reduced graphene oxide (rGO) cathodes have been explored for various battery systems, including Na–O_2, Li–CO_2, and Zn-air batteries. For instance, Qiao *et al* [86] introduced a novel method using 3DP to synthesize Ni nanoparticles anchored on an rGO framework (Ni/r-GO) via a heat-shocking process, enabling the fabrication of thick electrode designs for Li–CO_2 batteries (figure 8(a)). The ultrathick cathode, measuring 0.4 mm, was created in two stages: first, a GO framework was printed and then reduced in an argon gas environment to produce an rGO framework. Subsequently, the framework was immersed in a $NiCl_2$ solution, and ultra-fine Ni particles were thermally anchored onto the r-GO through a high-speed and high-temperature thermal-shocking process (figure 8(b)). The designed ultrathick electrode, along with the uniform dispersion of Ni nanoparticles, led to reduced overpotential and increased specific capacity (figure 8(c)). Similarly, Zhang *et al* [87] employed a direct ink writing (DIW) 3D printer to fabricate functional electrodes, including both anode and cathode, for Zn-air batteries. The printed freestanding air cathode exhibited a layered porous structure with characteristics such as a large surface area, strong electrocatalytic activity, and fast reaction-diffusion routes (figure 8(d)). Consequently, the constructed Zn-air battery demonstrated outstanding capacity (670 mAh·g^{-1}) and long-term stability (figure 8(e)).

3DP technology has revolutionized the fabrication of electrodes by enabling the production of precise and complex geometric structures in a highly automated and reproducible manner. One of the remarkable advancements in this field is the work by Ren *et al* [88], who introduced the use of CNT@MnO_2 ink synthesized through 3DP. By incorporating carbon nanotubes, they created a 3D network structure that improved conductivity and charge dynamics. Additionally, they replaced zinc foil with micron-sized zinc powder, resulting in a highly flexible battery device. This innovative approach allowed the electrodes to be separated by millimeters and directly in contact with the unitary electrolyte, reducing

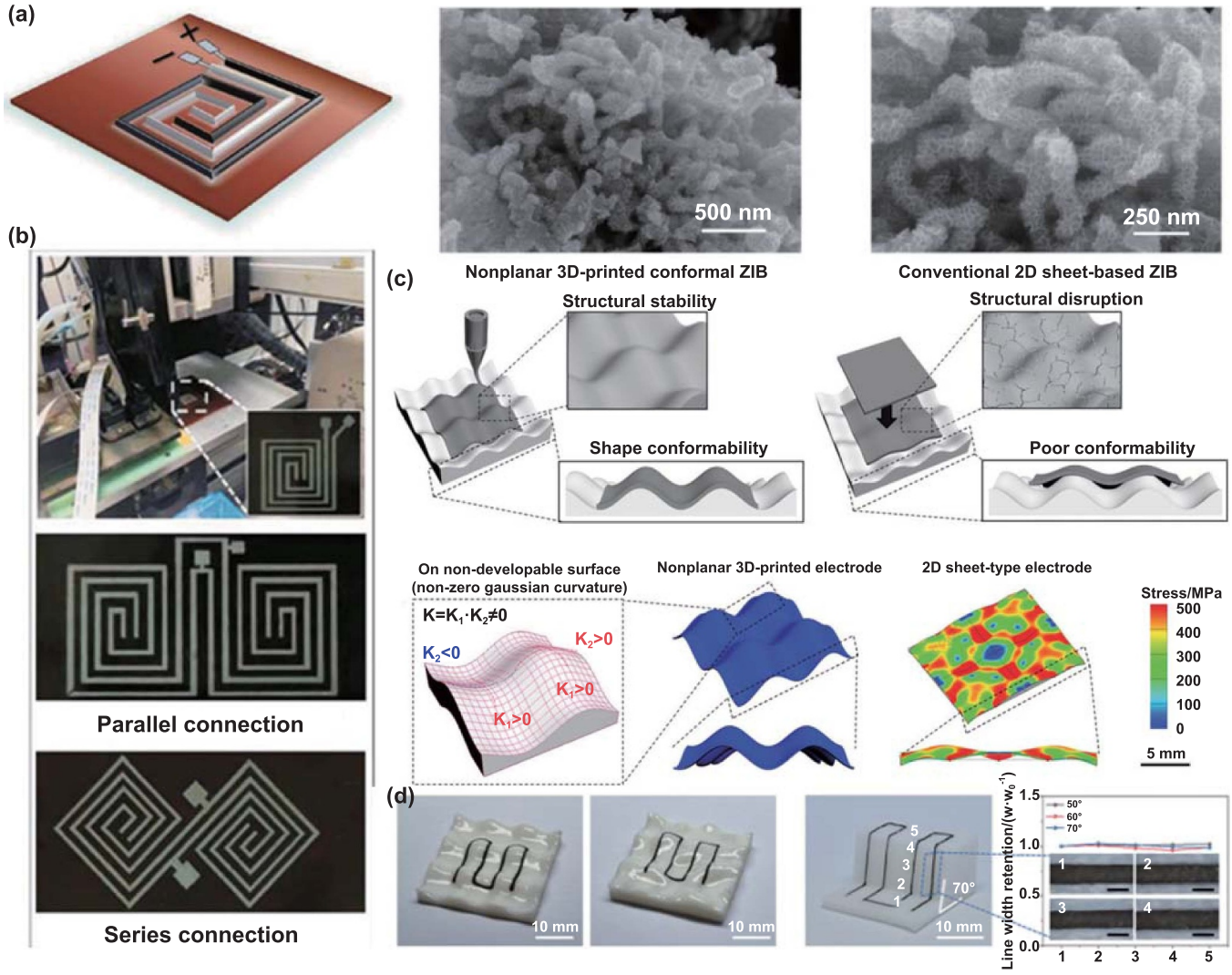

Figure 9. 3D-printed materials in ZIBs. (a) Schematic diagram of a 3D printing battery and SEM images of CNT@MnO_2. (b) Photograph of the multinozzle printing system. Reproduced from [88]. CC BY 4.0. (c) Schematic illustration of the fabrication of a conformal ZIBs using nonplanar 3D printing. (d) Photographs of the nonplanar 3D-printed cathodes on various 3D substrates. [89] John Wiley & Sons. [© 2023 Wiley-VCH GmbH].

dendrite penetration and enhancing ion transport. The 3D printed battery exhibited an impressive capacity of 63 μAh·cm^{-2} at 0.4 mA·cm^{-2}, while maintaining excellent performance even under different bending conditions, with a maximum change in capacity of only 2.72% (figures 9(a) and (b)).

Another notable contribution in the realm of 3D printed batteries is the work by Ahn *et al* [89], who developed a non-planar 3DP technique for ZIBs. Their approach involved the design of a ZIB component, comprising a Mansan-based cathode, a UV-curable gel composite electrolyte, and a zinc powder-based anode, using the DIW method. By carefully regulating the colloidal interaction within the ZIB component ink, they achieved a dual-infiltrated ion/electronic conduction pathway, ensuring efficient geometric synchronization with non-planar surfaces. The ZIBs fabricated using this approach demonstrated a high volumetric energy density, reaching 50.5 mWh·cm$_{cell}^{-3}$, thanks to their high-fill coefficient (figure 9). These remarkable advancements in 3D printed battery technology highlight the potential of this manufacturing technique for achieving enhanced performance, flexibility, and energy density. The ability to create intricate electrode structures and optimize material composition through 3DP opens up new avenues for the development of advanced energy storage systems.

In the past five years, there have been significant advancements in sulfur and carbon cathodes, paving the way for the exploration and development of high-specific-energy batteries. These advancements have attracted considerable attention and are expected to continue to be a focal point of research in the foreseeable future. Among the various manufacturing techniques employed in rechargeable batteries, DIW stands out as the most widely utilized method, accounting for 76.3% of all applications. It is followed by IJP and FDM. This widespread adoption of DIW can be attributed to its unique advantages, particularly its ability to work with a broad range of printable material precursors.

5. Structural design of anode materials

Since the commercialization of LIBs, the development of anode electrodes has become a crucial aspect in increasing their specific capacity. Graphite, the commonly used anode material, exhibits limitations such as insufficient capacity and poor rate performance, which are increasingly unable to meet the growing demands. The emergence of alternative battery systems, such as SIBs, potassium-ion batteries (KIBs), and ZIBs, provides an opportunity for diversifying energy storage options and filling the gaps in various applications.

To enhance the specific capacity of LIB anodes, various high-capacity materials have been successfully explored. These include carbon-based materials (such as graphene and hybrid materials), tin-based materials, silicon-based materials [90], titanium-based materials, and others [91]. Extensive research has been conducted to investigate 2D or 3D configurations that enable efficient Li^+ diffusion and achieve higher specific capacity and power.

Maurel *et al* described the formulation and characteristics of a 3D-printed graphite/polylactic acid (PLA) filament specifically designed for use as an LIB anode and compatible with standard commercial FDM 3D printers. Figure 10(a) [43] illustrates the optimized 10% CSP (graphite/conductive agent) film sample, which approaches theoretical capacity, and its corresponding filament used as a 3DP material supply. The most printable filament, 40% PEGDME500, exhibits good homogeneity, as confirmed by Raman microscopy analysis (figure 10(b)). The researchers successfully printed high-resolution complex 3D structures, such as a semicube lattice and a 3D boat (figure 10(c)). By studying various plasticizers, including PC, PEGDME2000, PEGDME500, and ATBC, their effects on thermal behavior and compatibility with composite films were investigated through DSC curves (figure 10(d)). The electrical conductivity was assessed by varying the ratio and content of conductive additives (figure 10(e)).

Lawes *et al* demonstrated the fabrication, optimization, and characterization of inkjet-printed (IJP) silicon (Si) anodes for LIBs [26] (figure 10(f)). Through a comparison of four polymer adhesives, they highlighted the importance of adhesives in achieving superior electrochemical performance of IJP Si electrodes. The self-healing effect was demonstrated using FTIR analysis based on the structure of PEDOT:PSS (figure 10(g)), which exhibited excellent performance and durability when used with the conductive polymer PEDOT:PSS adhesive (figure 10(h)). These studies highlight the advancements in developing anode materials for LIBs through 3DP techniques. By tailoring the composition, structure, and adhesive properties, researchers have been able to optimize the performance and durability of anodes, paving the way for improved energy storage capabilities.

For the fabrication of 3D electrodes, extrusion-based 3DP offers a potentially affordable and straightforward manufacturing solution. For instance, the FFF approach allows for downsizing and the design of free form factor batteries, as well as the reduction of dead mass components, the reduction of energy loss, the creation of a suitable interface, and an increase in the efficiency of energy transfer. Ragones *et al* described a unique concept and feasibility investigation of a 3DP FFF [92] (figures 11(a)–(c)). In cells using traditional liquid electrolytes, 3D printed $LiFePO_4$ (LFP) and lithium-titanium-oxide (LTO) composite polymer electrodes indicated reversible electrochemical reactions. This helped build a free-volume battery, reduce the volume changes that occur at the charging and discharging stages. The electrochemical activity of the electrodes proved that FFF-printed cells were technically feasible. While the method is promising for printing with thick electrodes, there is still a basic issue that has to be solved regarding the viability of the ink. Sun *et al* printed AgNWs, graphene, and $Li_4Ti_5O_{12}$ as highly conductive and hierarchical networks for mixed-function inks (figure 11(d)) [67, 92, 93]. The combination of conductive AgNW networks, linked 3D graphene scaffolds, and layered porous structures allows for significantly improved charge and ion transport, as well as reduced internal stress during ultra-thick charge–discharge operations, providing the necessary mechanical strength, which resulted in the enhanced stability (figure 11(e)).

The local current density and electric field concentration on the electrode are two extremely critical elements influencing the electrochemical behavior of $Li^+/Na^+/Zn^{2+}$ [72]. Conventional 2D planar anodes (bare Li, Na, Zn metal) have rough surfaces, contributing to non-uniform current distribution [70]. $Li^+/Na^+/Zn^{2+}$ preferred to electromigrate to tips when the local current density increased, which promoted dendrite formation [66]. Through 3DP, the structured Li/Na/Zn metal anode electrode can increase the SSA of the electrode, so that the total electric field was evenly distributed in the porous electrode, so as to decrease the current density, achieve uniform deposition, and inhibit volume changes of electrode, so as to enhance the cycle stability and safety [58, 65]. Increasing electrode thickness is a common method to increase battery areal capacity [27, 82]. However, due to basic difficulties such as insufficient electrolyte penetration, poor mechanical characteristics, and delayed charge and ion transport, the practical use of these thick electrodes is hampered. Continuous innovation as the foundation for creative advancement in quickly creating varied form-factor microelectronic devices necessitates smooth battery integrability [57, 94]. As a result, during the last decade, in terms of materials advancements for battery, the emphasis had shifted increasingly toward creative manufacturing techniques, unorthodox topologies, and multi-functional modules [68].

For Li metal anodes, such as graphene, CNTs, MoS_2-graphene, and MXenes, had been manufactured in the same way as the printed anodes of Li metal batteries. 3D-printed porous structures made of carbon, MXenes ($Ti_3C_2T_x$), and Cu, for instance, had been developed as hosts for the Li metal anode. According to the extrusion-type 3DP, shen *et al* developed a dendrite-free Li anode with a 10 mV overpotential, a 1200 h cycle life, and excellent areal capacities [95] (figure 12(a)). In 3DP anodes, MXene arrays with huge quantities of voids not only facilitated lithium nucleation, homogenized the electric field and lithium ion flow, successfully restrained the formation of Li dendrites, but also offered adequate room for the expansion of significant cobblestone lithium. V_2CT_x/rGO-CNT material is also fabricated by a

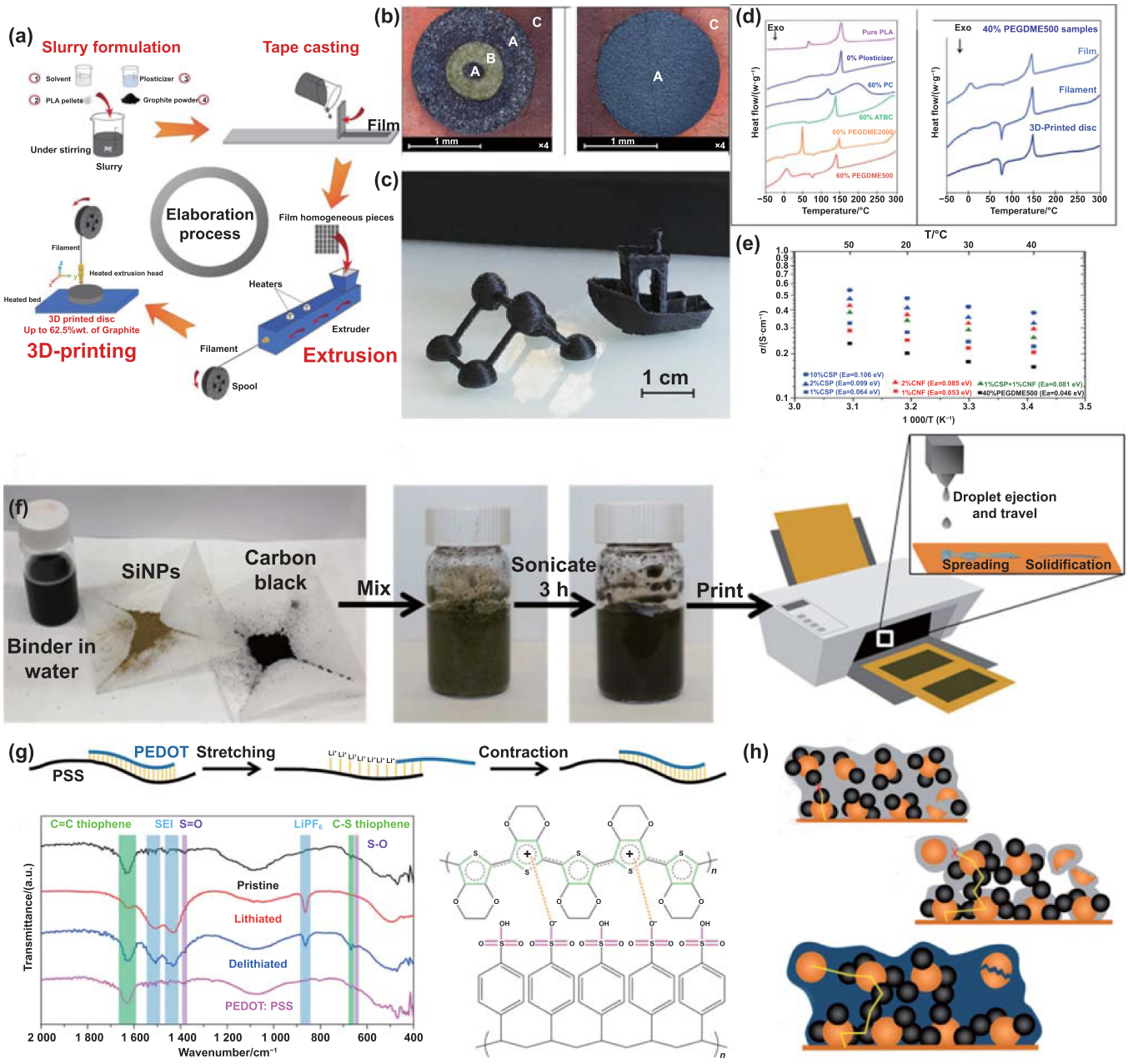

Figure 10. The applications of 3D-printed graphite-based and silicon-based anode materials in LIBs. (a) Procedures the 3DP graphite-based anode, (b) nonhomogeneous filament image obtained by optical microscopy of graphite and PLA, (c) optical image of 3D objects printed by 40% PEGDME500, (d) DSC curves for various printed disc, and (e) Arrhenius plots of the electrical conductivity for various samples. Reprinted with permission from [43]. Copyright (2018) American Chemical Society. (f) Optical diagram of preparing printing ink of Si anode and mechanism analysis of 3D-Si electrode. (g) FTIR spectra of SiNP anodes with PEDOT:PSS binder taken at three stages, and schematic structure of PEDOT:PSS. (h) Schematic illustration of the proposed mechanism to electrochemical performance of anodes with various binders. Reprinted from [26], Copyright (2017), with permission from Elsevier.

DIW 3DP technology and further adopted as the matrix of Na metal. The 3D-printed V_2CT_x/rGO-CNT aerogel was demonstrated to be superior matrix for Na metal anodes due to the large specific surface area and sodiophilic V_2CT_x MXene nanoflakes [55] (figure 12(b)). 3D hierarchical porous flexible Zn anode (3DP-ZA) was printed for the first time by a component in the formulated ink (CNT, graphene and cellulose) [61]. In this design, 3DP technology plays a vital role in fabricating the flexible Zn anode, and tight integration among carbon matrix, Zn powder and zincophilic Ag particles gurantees a good flexibility and structural stablility, which shows huge potential for the practical application of flexible ZIBs (figure 12(c)).

Furthermore, 3DP technology has been utilized to address crucial challenges associated with Li metal anodes by employing MOF-based materials and biomass materials. These materials aim to mitigate issues such as uncontrolled Li dendrite formation and significant interface changes. Lyu *et al* achieved

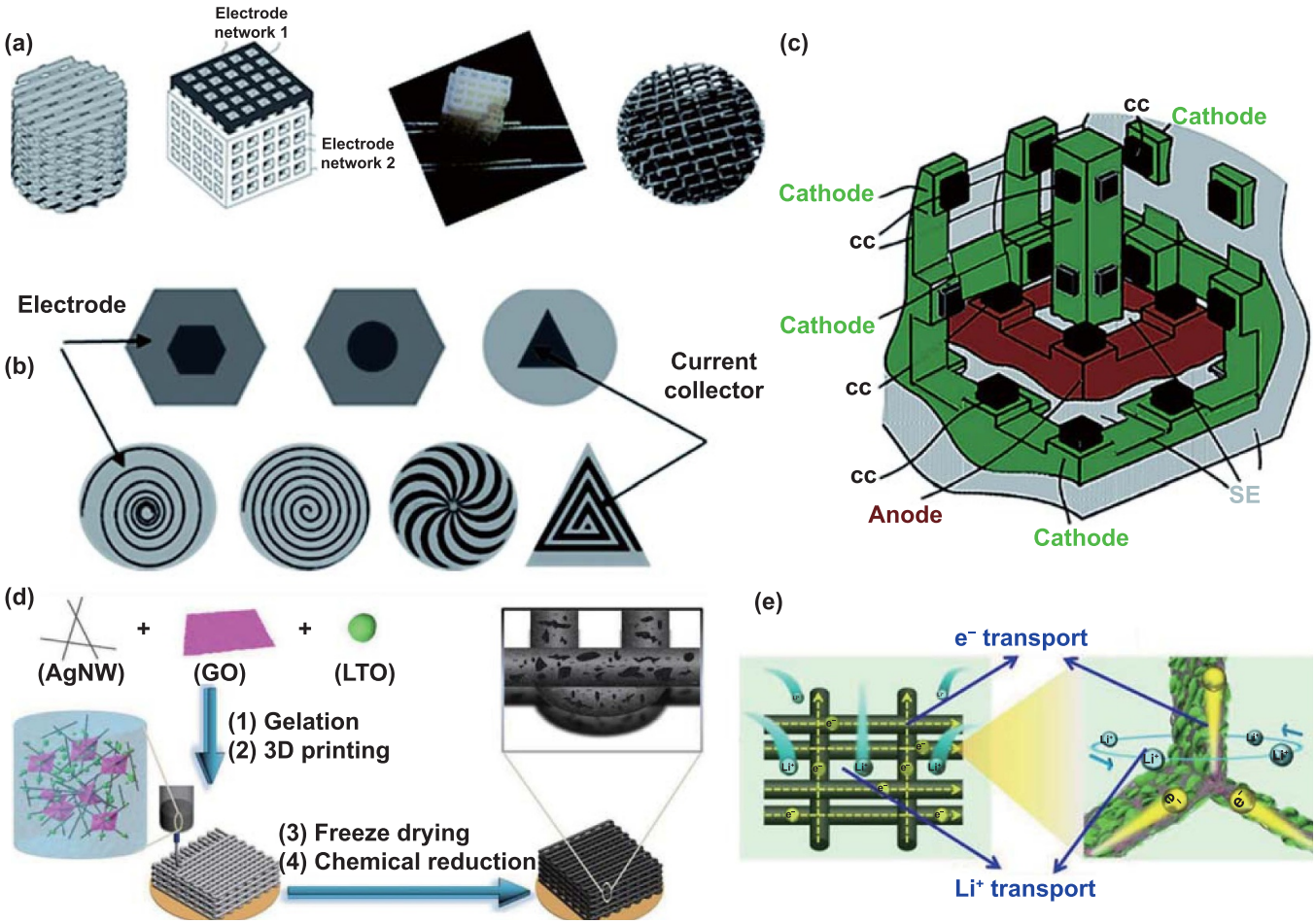

Figure 11. The application of extrusion-based 3D printing technology in 3D electrodes design. (a) Schematics and models of 3DP various electrodes; (b) the structure design of 3D batteries and (c) overall view. Reproduced from [92] with permission from the Royal Society of Chemistry. (d) Diagram of the fabricating rGO-AgNWs-LTO cells and (e) mechanism analysis. Reprinted from [67], Copyright (2020), with permission from Elsevier.

a breakthrough by 3DP a unique N-doped carbon framework with a hierarchically porous host and high surface area using an extrusion-based Zn-MOF precursor (figure 13(a)) [94]. The distinctive structural characteristics of the framework effectively inhibited dendrite formation, facilitated Li plating, stabilized the Li/electrolyte interfaces, and promoted high local current dispersion.

In another pioneering study, Cao *et al* successfully employed cellulose nanofiber (CNF), one of the most abundant biopolymers on Earth, to fabricate high-performance lithium metal batteries (LMBs) through 3DP [58] (figure 13(b)). The researchers demonstrated the 3DP of cathode and anode scaffolds, as well as the rheological properties of the inks, and developed CNF/LFP samples with varying layers (figure 13(c)). The incorporation of CNF gel in the printing process provided a stable framework for Li deposition alongside the LFP electrode. The feasibility of the CNF gel was thoroughly investigated, and the permeable design of CNF scaffolds enhanced ion permeability while reducing local current density during Li plating. As a result, dendritic formation caused by uneven Li plating or stripping was significantly reduced. Figure 13(d) showcases the initial assembly of a fully packed LMB with 3D-printed electrodes, which effectively powered a LED light with a working voltage exceeding 3.0 V. Moreover, a multiscale numerical technique incorporating first-principle theory and a multi-physical field model revealed that the porous structures exhibited more homogeneous Li deposition (figure 13(e)).

Considerable research has been dedicated to the advancement of a wide range of cathode and anode materials, as exemplified by the sample printed batteries presented in table 2. The utilization of 3DP technologies holds great promise in fabricating crucial components for rechargeable batteries, offering exceptional adaptability and enabling high mass loadings. This approach has the potential to significantly enhance areal capacities and energy densities. Through the precise control afforded by 3DP, various materials and processes have been explored, leading to the creation of innovative battery architectures. These advancements contribute to the continuous improvement of battery performance and the realization of more efficient and sustainable energy storage systems. The integration of 3DP techniques with battery technology opens up exciting avenues for future research and development in the field of electrochemical energy storage.

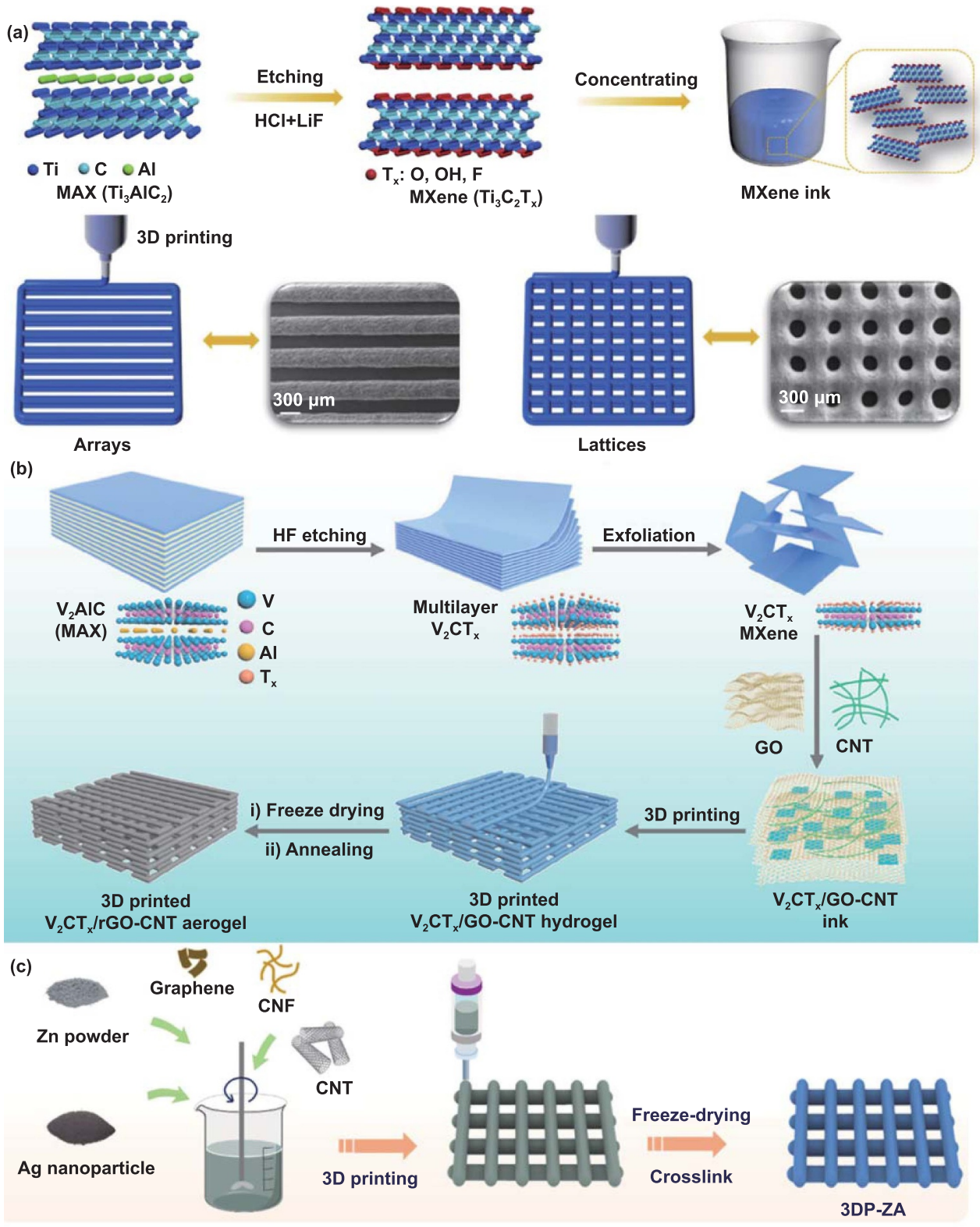

Figure 12. 3D-printed various 3D hosts for metal anode batteries. (a) Diagram of preparing raw $Ti_3C_2T_x$ MXene, 3D MXene electrode, and the morphology of Li plating. Reprinted from [95], Copyright (2020), with permission from Elsevier. (b) Procedures of fabricating 3D V_2CT_x/rGO-CNT aerogel for Na metal anode. Reprinted with permission from [55] Copyright (2022) American Chemical Society and (c) 3D printing Ag anchored hierarchical porous flexible Zn anode. Reprinted from [61], Copyright (2023), with permission from Elsevier.

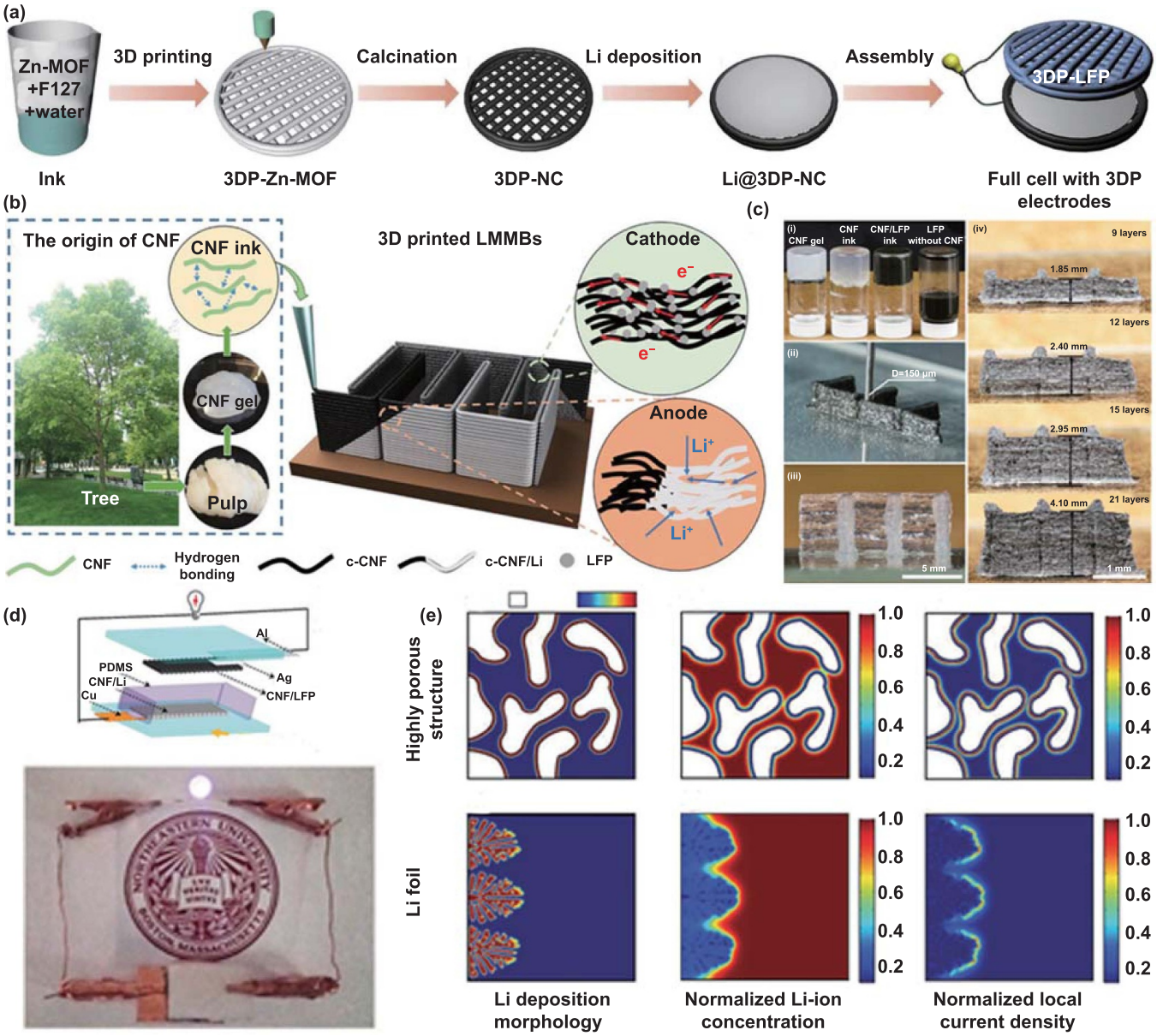

Figure 13. 3D-printed carbon-based hosts for Li metal anodes. Diagram of (a) the Li plating process on 3D-printed carbon-based hosts. Reprinted from [94], Copyright (2020), with permission from Elsevier and (b) 3D printed c-CNF scaffolds for LMMBs; (c) optical image of pristine dispersions, CNF/LFP cathodes printed one layer after another. (d) The illustration of 3D-printed cell structure, and LMBs powering a white LED lamp. (e) Theoretical simulations of Li plating morphologies, normalized Li^+ ion concentration, and local current densities. [58] John Wiley & Sons. [© 2019 WILEY-VCH Verlag GmbH & Co. KGaA, Weinheim].

6. Separator/electrolyte

In addition to the anode and cathode, the separator/electrolyte plays a crucial role in rechargeable batteries [115]. The interface between the separator/electrolyte and the electrodes is particularly important as it significantly influences the electrochemical performance. In this regard, 3DP offers a viable approach for interface design by allowing the adjustment and fabrication of the separator/electrolyte morphology.

The separator must possess uniform pore-size distributions, excellent thermal and mechanical stability, as well as remarkable electrochemical stability, which have been extensively studied in conventional rechargeable batteries [104, 116–118]. However, printing the separator remains a challenging task [119], and further research is needed to assess whether printing can enhance its performance [94, 120, 121]. Recently, solid-state rechargeable batteries have garnered significant attention due to their stability and safety advantages. SSEs offer improved safety, increased energy densities, potential enhancements in cycling lifespan, and fast-charging capabilities [122, 123]. To meet the requirements of emerging markets, advancements in solid electrolyte materials are necessary, along with the rapid progress in 3DP techniques [31, 124].

Table 2. Summary and comparison of the various kinds of methods and materials for 3D-printed rechargeable batteries.

Printing method	Cathode/anode	Specific capacity/(mAh·g^{-1})	Current density/rate	Battery type	References
Fused deposition modeling	Li foil/(graphene/PLA)	40	120 C	LMBs	[96]
	Pt/graphene	248	40 mA·g^{-1}	—	[97]
	Li/(graphite/PLA)	215	18.6 mA·g^{-1}	LMBs	[43]
	(lithium manganese oxide/MWNTs)/(lithium titanate, graphene nano-platelets)	7.48 mAh·cm^{-3}	1 C	LIBs	[92]
	(LFP/graphite/MWNTs) (LTO/carbon/polyester polylactic acid)	80	2 C	LIBs	[98]
Lithography-based 3D printing	(LMO/NiSn)	≈2.9 μAh·cm^{-2}·μm^{-1}	1 C	—	[99]
	LFP/$LiTiO_2$	500 mAh·cm^{-2}	0.1 C	LIBs	[100]
	LFP/LTO	1.4 μAh·cm^{-2}	2 C	LIBs	[101]
Aerosol jet printing	LFP/(Li foil)	151	0.067 C	LMBs	[102]
Direct ink writing	($Na_3V_2(PO_4)_3$ graphene oxide)/($Na_3V_2(PO_4)_3$ graphene oxide)	1.26 mAh·cm^{-2}	0.2 C	SIBs	[103]
	(CNF/LFP)/(CNF/Li)	140	0.2 C	LMBs	[58]
	LFP/LTO	133	0.2 mA·cm^{-2}	LIBs	[83]
	LFP/LTO	1.5 mAh·cm^{-2}	5 C	LIBs	[30]
	(S/GO/DIB)/(Li foil)	812.8	—	LMBs	[86]
	(Ni/rGO)/(Li foil)	1000	100 mA·g^{-1}	LMBs	[63]
	LFP/LTO	10	50 mA·g^{-1}	LIBs	[29]
	(LFP/CNF/PVDF)/(LTO/CNF/PVDF)	154	0.2 C	LIBs	[104]
	(LFP/$LiCoO_2$)/(LTO/CNF/PVDF)	150	0.2 C	LIBs	[74]
	MnO_2/Zn	0.98 mAh·cm^{-2}	—	ZIBs	[75]
	MnO_2/(Li foil)	127.3	—	LMBs	[105]
	hGO/(Li foil)	13.3 mAh·cm^{-2}	0.1 mA·cm^{-2}	LMBs	[106]
	(LTO/GO)/(LTO/GO)	185	10 mA·g^{-1}	—	[15]
	(S/BP2000)/(Li foil)	1009	5.5 mg·cm^{-2}	LMBs	[76]
	(LFP/AB/CNT)/(LFP/AB/CNT)	150	0.1 C	—	[41]
	LFP/LTO	128	0.2 C	LIBs	[107]
	(NC-Co)/(Li foil)	525	0.8 mA·cm^{-2}	LMBs	[85]
	(carbon black/$MnCo_2O_4$/rGO/CNT)/Zn	142.8 Ah·l^{-1}	0.1 mA·cm^{-2}	ZIBs	[108]
Inkjet printing	$LiMn_{0.21}Fe_{0.79}PO_4$@C/(Li foil)	150.21	10 C	LMBs	[66]
	LFP Composite/(Li foil)	150	1 C	LMBs	[81]
	(Na disk)/(Hybrid MoS_2–graphene aerogel)	429	3.3 C	SIBs	[66]
	Li/SnO_2	812.7	1 C	—	[109]
	LFP/(Li foil)	134.7	0.1 C	LMBs	[110]
	MWCNT/(Li foil)	1260	0.5 C	LMBs	[102]
	$LiCoO_2$/(Li foil)	105	394 μA·cm^{-2}	LMBs	[111]
	S/Li–S/(Li foil)@SWNT	850	0.5 C	LMBs	[112]
	Li foil/(Si NPs/PEDOT:PSS)	2500	0.1 C	—	[113]
	$Li_{1.2+x}Mn_{0.54}Ni_{0.13}$ $Co_{0.13}O_2$/(Li foil)	>250	0.1 C	LMBs	[114]
	LFP/Li4TisO12	60	0.1 C	LIBs	[26]

A variety of 3D-printed electrolytes have been reported for SSE, including polymers [29, 125, 126], ceramics [98, 127–129], and polymer-ceramic hybrids [130–134]. Unlike conventional manufacturing processes, the printability of electrolytes is a critical characteristic for 3DP. Currently, DIW is widely employed in 3DP electrolytes due to its wide selection of printable inks. Additionally, SLA is used to achieve high-resolution and complex structures using photocurable inks. Generally, 3DP electrolyte inks comprise polymer substrates, salts, and additive fillers. The ink is extruded or stacked during the 3DP process, with the polymer substrate determining strain behaviors such as rheological properties, shear, and yield. Commonly used polymer substrates in 3DP electrolyte inks include polyvinylidene fluoride (PVDF), polyethylene oxide (PEO), and their copolymers. Based on these techniques and materials, several design principles have been discussed.

One of the key design principles focuses on the electrolyte–electrode interfaces. In solid-state batteries, a major challenge is the high intrinsic resistance resulting from insufficient contact at the electrolyte–electrode interfaces. 3DP enables the optimization and patterning of interlocks between the electrolyte and electrode [135, 136]. Printing structured polymers or ceramics proves to be an effective approach for achieving strong interfaces. For instance, He *et al* utilized SLA to print a 3D Archimedean spiral structure using a PEO-based electrolyte [137] (figure 14(a)). A precursor surface was initially formed using a laser, and then the wavelength was shifted over the precursor surface according to the planned models. After each layer had solidified, the stage was lowered downward. Compared to conventional electrolytes, the structured solid polymer electrolyte exhibited shortened ion transport paths into the electrodes (figure 14(b)) due to the strong adherence between the interfaces. These structured polymers resulted in lower resistances (394 Ω at 50 °C, 1705 Ω at 25 °C), higher capacity retention (77% after 250 cycles), and improved cycling stability, as shown in figure 14(c). Similarly, strong interfaces were achieved through 3DP for fabricating ceramic electrolytes. McOwen *et al* employed DIW to create a thin, nonplanar, intricate ceramic grid composed of $Li_7La_3Zr_2O_{12}$ (LLZO) scaffold [29] (figure 14(d)). With the Li metal immersion and coverage, the contact area between LLZO and Li significantly increased, demonstrating good interface contact and stable cycling capability. By varying the current densities from 0.1 to 0.33 $mA{\cdot}cm^{-2}$, the average overpotential was measured as 2.3 mV and 7.2 mV, respectively, corresponding to an extremely lower area-specific resistance of 22 $\Omega{\cdot}cm^2$ (figure 14(e)).

Overall, these advancements highlight the potential of 3DP techniques for designing and fabricating electrolyte–electrode interfaces in solid-state batteries. By employing tailored structures and materials, 3DP offers a promising avenue for improving the performance and reliability of SSEs, ultimately contributing to the advancement of next-generation rechargeable battery technologies.

In addition to the adjustable electrolyte–electrode interfaces, another designing principle for 3DP electrolytes involves balancing and improving performance. The advancement of suitable solid electrolytes with strong ionic conductivity and adequate mechanical characteristics is one of the main issues [27, 138]. While polymer electrolytes typically have limited ionic conductivity, ceramic electrolytes have poor mechanical characteristics [139, 140]. Hence, there is an increasing amount of interest in polymer-ceramic hybrids. Conventional processing techniques cannot easily fabricate sacrificial and complex templates [141, 142]. 3DP addressed this issue by not only providing the tunable material ratio but also possessing automatable preparation process. Blake *et al* employed DIW in a so-called dry phase inversion method to develop a novel electrolyte with controlled porosity [104]. The printing ink consisted of several combinations of NMP, PVDF, glycerol, and Al_2O_3 nanoparticles (figure 15(a)). Using different precursors, various electrolyte materials can be printed (figure 15(b)). The introduction of the dual-solvent system yielded high porosity (with large voids around 5 μm). Since phase inversion was not employed to create a porous structure, the obtained morphology seemed denser when Al_2O_3 particles and PVDF were added to NMP without glycerol (CPE). With an optimized polymer/ceramic ratio ($PVDF/Al_2O_3 = 30/70$) in the dual solvent, a higher specific area (17 $m^2{\cdot}g^{-1}$) was abstained, suggested that Li^+ transport routes may have been affected upon by the preservation of void space between nanoparticles (CPE-PI). Among that, enhanced flexibility and electrochemical performance can be realized through tunable 3DP conditions. Hence, in order to meet printing requirements, it is feasible to adjust the electrolyte's ionic conductivity, mechanical stability, and thermal characteristics as well as the rheology of the inks. The optimized porous hybrid electrolyte CPE-PI showed higher specific capacity than the bulk mixed electrolyte CPE at different rates (figure 15(c)). Meanwhile, at 0.2 C, the PE-PI, CPE, and CPE-PI failed at 85 h, 500 h, and over 4000 h, respectively. The cycle performance of CPE-PI exceeded that of commercial membranes (failed at 3400 h) which demonstrated the effectiveness of the 3DP technique in optimizing electrolyte materials.

Besides the polymer/ceramics ratio, 3DP can also enable the unique hybrid architecture of the polymer and ceramic components [62, 122]. Zekoll *et al* presented 3D-ordered bi-continuous structures of hybrid solid electrolytes [31]. Through SLA, a printed template was first obtained. Following by filling with ceramic Li^+ conductor $Li_{1.4}Al_{0.4}Ge_{1.6}(PO_4)_3$ and removing the initial templates by calcination at 900 °C, a LAGP ceramic scaffold was constructed. Finally, the structured hybrid electrolyte is produced by covering the bare scaffold with non-conducting polypropylene or epoxy polymer (figure 15(d)). The distinctive microarchitecture provided the optimum balance of conductivity and mechanical characteristics. Therefore, a wide range of particular hybrid microstructures, including cubic, gyroidal, diamond, and spinodal structures, may be accurately created (figure 15(e)).

Up to now, several promising 3DP technologies (DIW [128, 131, 134], SLA [125, 130], FDM [126, 133]) have been employed in the development of separators and solid electrolytes [143–145]. The majority of current research is on the development of stable, high-ionic conductivity solid

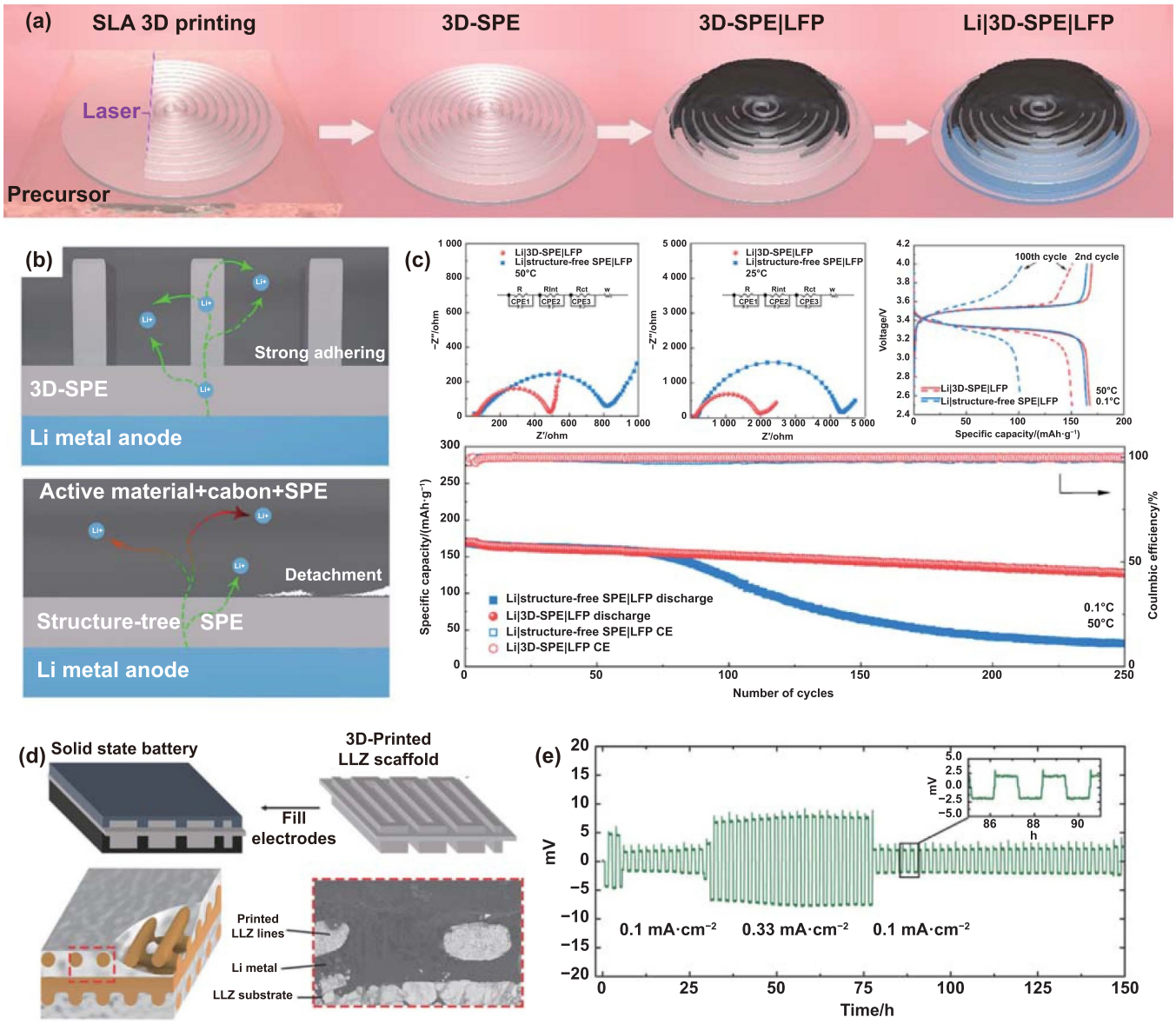

Figure 14. 3D printing technique on polymer/ceramic electrolytes. (a) Print polymers onto laser-curves surface to achieve 3D-SPE by SLA. (b) The electrodeposition process and (c) battery performance of 3D-SPE and structure-free SPE. Reprinted with permission from [137]. Copyright (2020) American Chemical Society. (d) The DIW process, obtained interfaces between structured LLZ and Li, and (e) the corresponding cycling performances. [29] John Wiley & Sons. [© 2018 WILEY-VCH Verlag GmbH & Co. KGaA, Weinheim].

electrolytes [146, 147]. The advantages of 3DP for solid electrolytes includes internal interlocking and stable interfaces, which is more conducive to low impedance and cycle stability. In the near future, several optimized strategies regarding 3DP separator/electrolyte should be given more attention and research. In order to obtain appropriate viscosity and rheological properties, more printable materials besides PVdF and PEO-based inks and suitable additives can be developed in the future. Furthermore, more 3DP techniques should be introduced in addition to DIW to achieve higher printing accuracy and processing efficiency. In addition, the designing principles of 3DP separator/electrolyte should be studied more comprehensively and systematically. Based on the existed cylindrical, grid, and matrix geometries, different microarchitectures, materials, and interfaces should be explored, and the mechanism of performance improvement should be further clarified.

7. 3D-printed hosts

In recent years, 3D hosts have been increasingly applied and discussed, which was seen as additional components. This involves the performance improvement of rechargeable batteries. It is considered that rechargeable batteries, especially metal-ion batteries, suffer from unsatisfactory cycling stability [148]. The low cycling lifetime stems from the growth of dendrite and undesired side reactions on conventional metal foil electrodes [137, 142, 149]. The metal ions thermodynamically preferred to nucleate on the pristine defects and

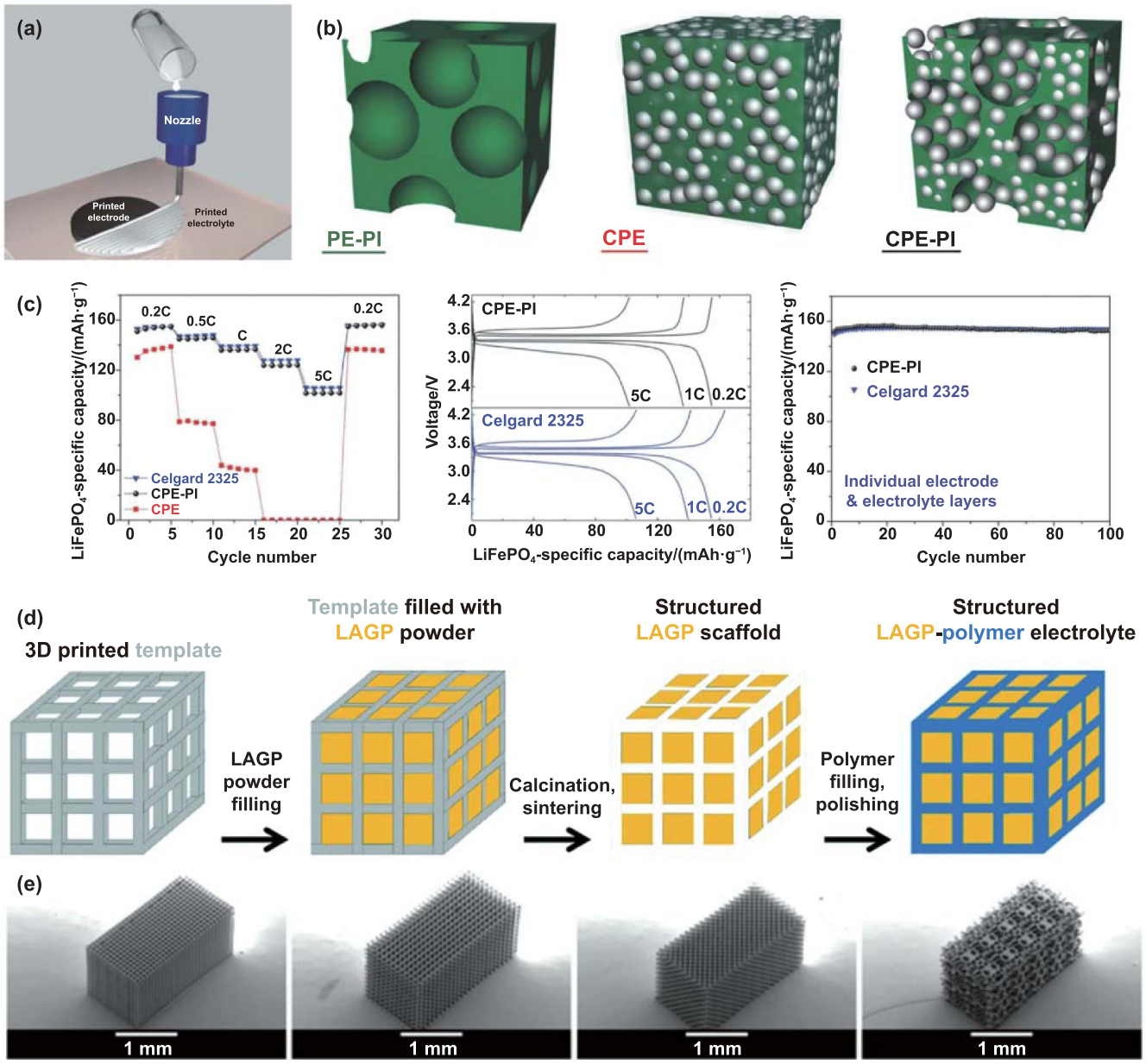

Figure 15. 3D printing technique on hybrid electrolytes. (a) The typical DIW process, (b) the obtained different electrolytes (porous PVDF, bulk and porous Al_2O_3/PVDF hybrid electrolytes), and (c) corresponding battery performances. [104] John Wiley & Sons. [© 2017 WILEY-VCH Verlag GmbH & Co. KGaA, Weinheim]. (d) The SLA processes and (e) different printed hybrid microstructures include cubic, gyroidal, diamond, and spinodal structures. Reproduced from [31] with permission from the Royal Society of Chemistry.

uneven surfaces of the metal foils [150, 151]. Moreover, the low-mechanical-strength fibrous separators, which have poor cycle performance, poor rate capability, low coulombic efficiency, and disabled electrochemical devices, are readily deformed by the sharp dendrites [135, 152, 153]. The development of metal dendrites has been inhibited using a variety of techniques, including electrolyte tuning, SEI layer alteration, and 3D structure creation [154–156]. All in all, using 3D hosts has been shown to successfully stop metal dendrite formation. As demonstrated in [83, 145], zinc [157, 158], sodium batteries [150, 159], the higher specific surface areas of 3D hosts can lower local current densities and homogenize interface charge distributions, enabling uniform plating of metal ions. The technology and material choices for 3D hosts are relatively diverse. Generally speaking, carbon-containing (including graphene and carbon nanotubes) and metal-containing printable inks are commonly selected for DIW and DLP.

To satisfy the actual needs of 3D hosts, 3DP is an efficient method for fabricating arbitrary shape [160–162]. DIW is one of the most common 3DP methods for hosts [151–153]. Lyu *et al* presented 3D-printed grids for Li deposition [94]. A solution dissolving Zn-MOF and F127 was used as the printing ink. In order to pressurize the syringe and regulate the ink discharge speed, a compressed air pneumatic device was employed (figure 16(a)). As 3D hosts for Li metal, the large-sized microchannels produced by 3DP fibers assisted in accommodating a massive Li plating and

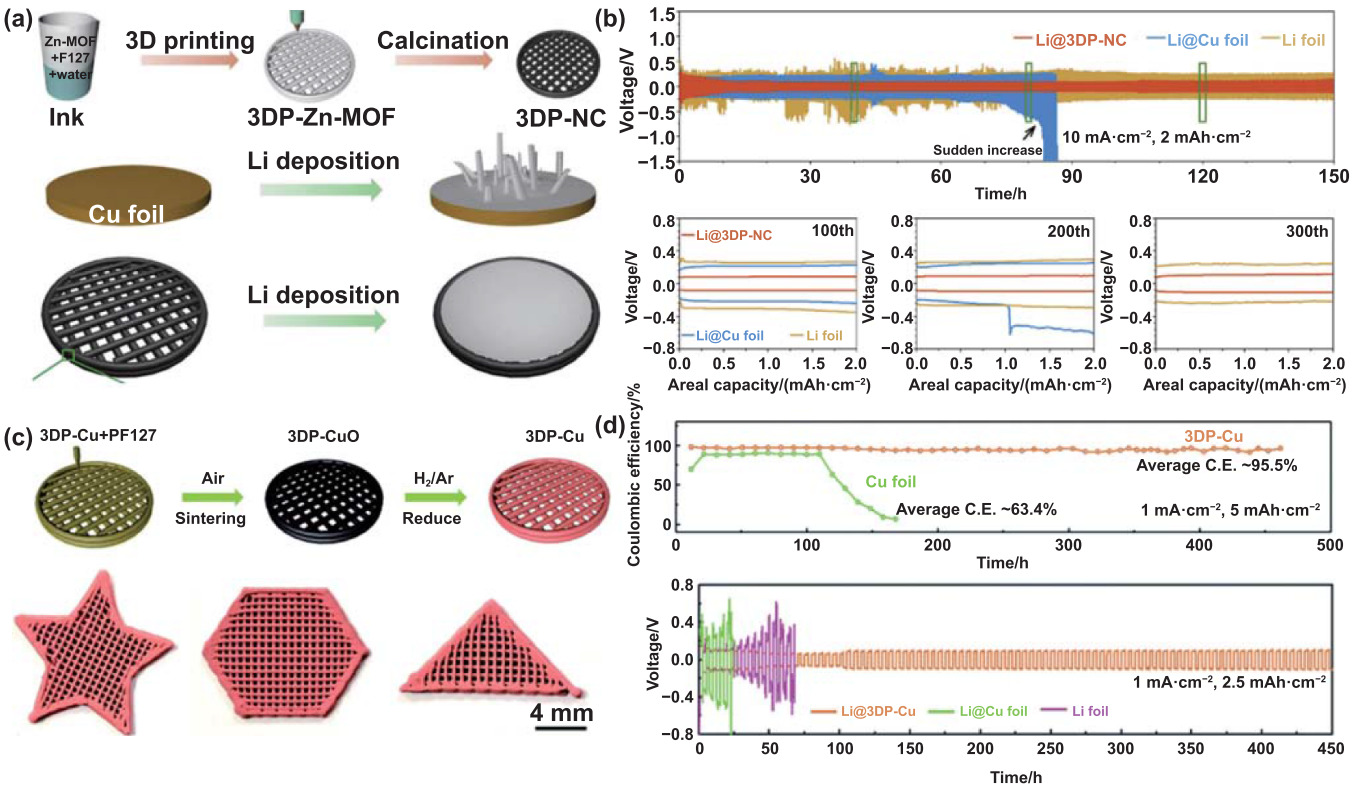

Figure 16. 3D hosts through DIW. (a) The typical DIW process to fabricate 3D hosts, the schematic of dendrite growth on Cu foil and 3D hosts, and (b) the corresponding battery performances. Reprinted from [94], Copyright (2020), with permission from Elsevier. (c) The different 3D hosts with various shapes and sizes processed by DIW and (d) the comparison between batteries with and without printed hosts. Reproduced from [27] with permission from the Royal Society of Chemistry.

suppressing Li metal volume changes. Within 150 h of cycling at 10 mA·cm^{-2} and 2 mAh·cm^{-2}, the large surface area had dispersed the low overpotential of 80 mV (figure 16(b)). Owing to the highly tunable and precisely developed DIW technique, Lim *et al* demonstrated that replicable and complex structures of variety-shaped 3D hosts could be fabricated [27] (figure 16(c)), The Li-metal battery with 3D Cu host exhibited average columbic efficiency at 95.5% within 450 h at a high areal capacity, and the 3D printed host enabled longer cycling times from lower than 75 h (without hosts) to 450 h (figure 16(d)).

Other than that, the DLP technique is also adopted for 3D host fabrication [157, 158]. Zeng *et al* [158] demonstrated a UV SLA 3D printer by hardening UV photosensitive epoxy. Because of the advanced electroless plating method and the strong binding energy of the zinc atom and the Ni surface, Ni was selected as the metalized coating. The 3D multichannel Ni–Zn lattices were fabricated as optimized zinc anodes with 3D architecture and robust supporting skeletons via electrodeposition Zn metal on the surfaces of 3D-Ni (figure 17(a)) [54]. At different current densities, 3D structured hosts showed higher capacity compared with 2D hosts during charging and discharging. Furthermore, higher capacity retention (80%) compared to conventional hosts battery (67%) after 1000 cycles was obtained (figure 17(b)). Through DLP, different morphologies were achieved and the metal deposition hosting effects could be optimized [163, 164]. Wu *et al*, for example, suggested 3DP graphene tube (3DGT) and pillar (3DGP) structures for ZIBs via DLP (figure 17(c)) [119]. According to multi-physical simulation, the 3DGT structured hosts enabled more uniform deposition and hence reduced the stress on the separator compared to 3DGP structures (figure 17(d)). Under 2 mA·cm^{-2} and 1 mAh·cm^{-2}, the 3DGT-based zinc symmetric cell exhibited the lowest overpotential at 14.0 mV and the longest cycling time at 1100 h (figure 17(e)). It showed that the 3DGT indicated greater advantages in reversible Zn depositing/stripping than the 3DGP and 2D commercial Zn foils.

8. 3D printed microelectromechanical systems (MEMS)

MEMS, also referred to as micro-electro-mechanical systems, micro-systems, or micro-machines, are advanced devices that can be measured in millimeters or smaller. The internal structure of MEMS typically ranges in size from microns to even nanometers, rendering them self-contained intelligent systems. Accelerometers, inkjet heads, pressure sensors, and gyro sensors are commonly utilized in MEMS. While silicon (Si) materials have traditionally served as the foundation for MEMS devices, polymers have emerged as alternative materials in recent years. Examples include polydimethylsiloxane for microfluidic devices, parylene for valves and sensors, and epoxy for micromanipulators.

Figure 18(a) illustrates the integration of 3DP technology with MEMS for robotic handling, featuring an integrated pick-and-place functionality [165]. Lee *et al* achieved a switch

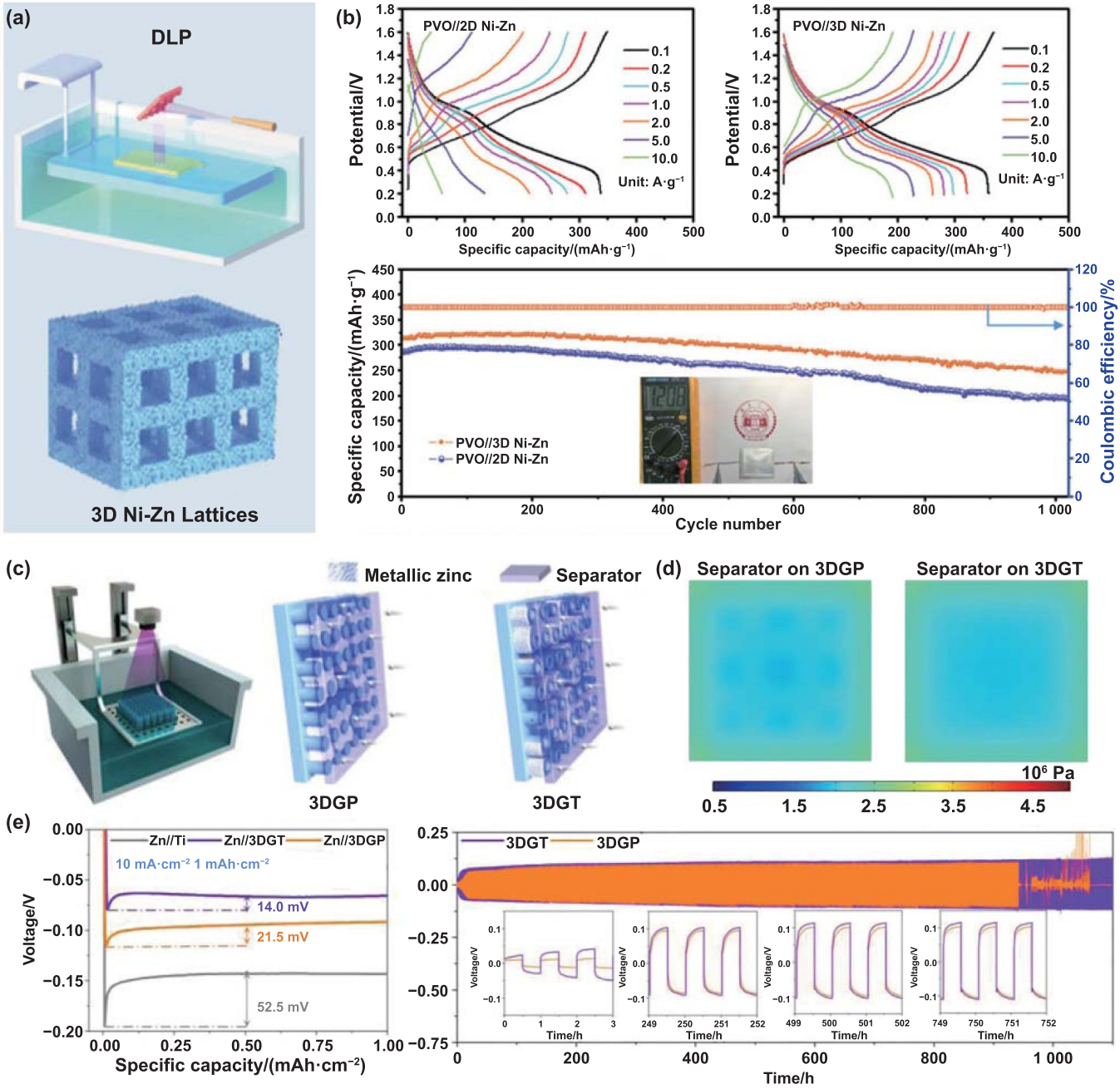

Figure 17. 3D hosts through DLP. (a) The typical DLP process for printing lattice structure and (b) the corresponding cycling performances. [54] John Wiley & Sons. [© 2021 Wiley-VCH GmbH]. (c) The DLP process for printing 3D pillar hosts and 3D tube hosts. (d) The simulated electrochemical deposition on different host configurations and (e) the experimental battery performances. Reprinted from [119], Copyright (2023), with permission from Elsevier.

with excellent electrochemical properties, abrupt switching behavior, and a high on/off current ratio exceeding 106 using FDM printing of conductive PLA and poly(vinyl alcohol) as a water-soluble support material (figure 18(b)). Additionally, an interdigitated 3D microbattery offers several unique attributes for on-chip energy storage. Ning *et al*'s group fabricated mesostructured electrodes by combining 3D holographic lithography with conventional photolithography techniques (figure 18(c)). The optical and SEM images of the 3D printed electrodes, as depicted in figure 18(d), demonstrate precise machining and novel structural design. The flexibility in designing holographic structures was achieved by manipulating the intensity, polarization, and angle of each beam, resulting in high power and energy densities (6.5 μWh·cm^{-2}·μm^{-1}). The flexibility, energy capacity, and power of microbatteries are closely associated with the structural parameters of the 3D-printed electrodes, including size, shape, surface area, porosity, and tortuosity. The goal of MEMS development is to explore new principles, functional components, and systems through miniaturization and integration, leading to the emergence of new technological fields and industries. The combination of MEMS and 3DP technology

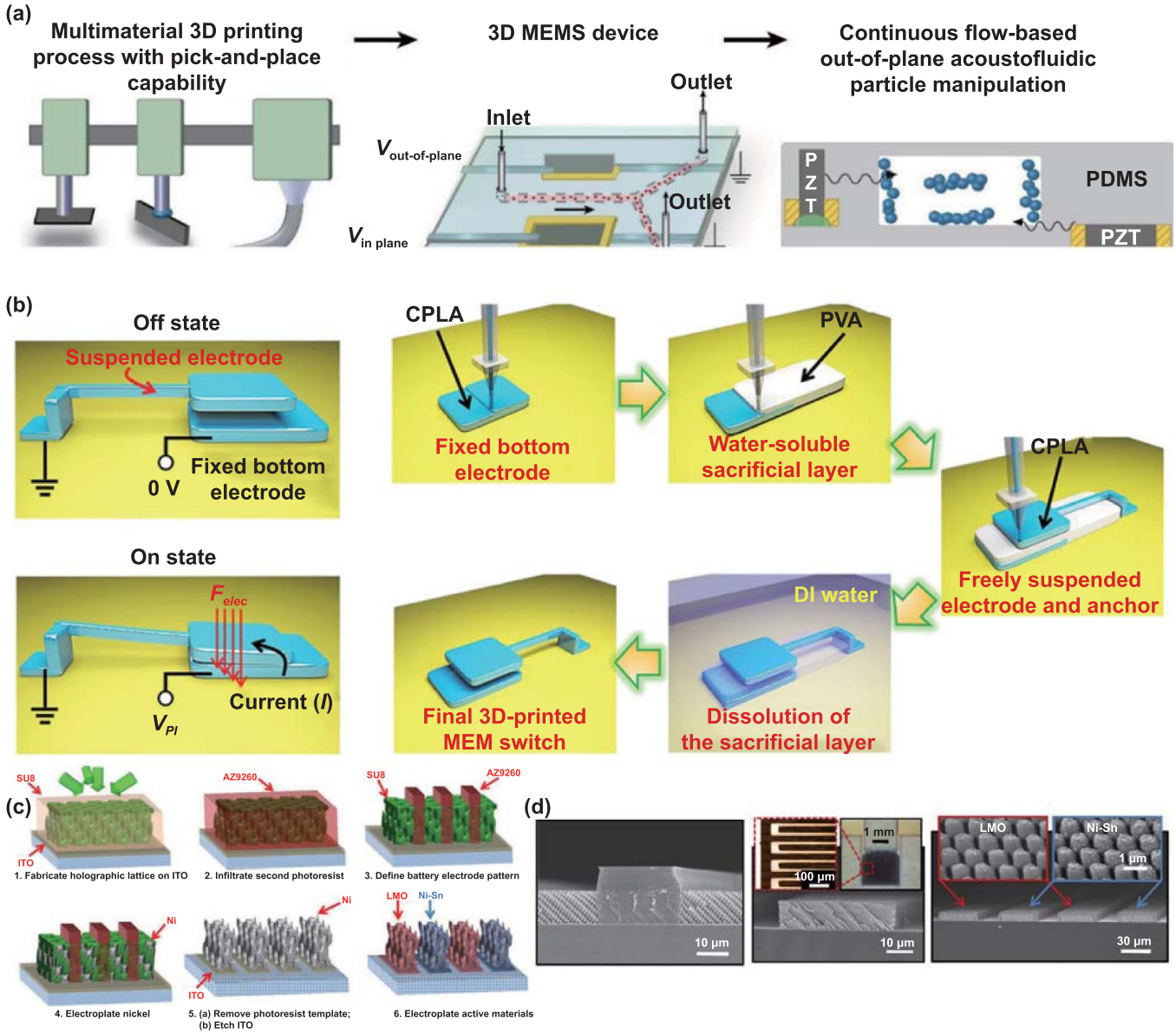

Figure 18. The integration of 3D printing technology with MEMS. (a) Combination of 3D printing and pick-and-place functionality to produce 3D MEMS devices. (b) Concept of 3D-printed MEMS switch and printing process. Reproduced from [165]. CC BY 4.0. (c) Schematic illustrations and images of 3D microbatteries, and (d) SEM and optical images of the 3D printed structures. Reproduced from [166]. CC BY 3.0.

offers novel opportunities for the development of microbatteries for new energy applications.

Based on the aforementioned discussion, 3DP technologies offer distinct advantages for producing rechargeable batteries, such as customizable morphology, effective dendrite suppression, and longer cycle life. However, optimizing the mechanical stability of 3D-printed hosts is crucial due to its direct impact on the battery's practical lifespan. Additionally, the design of 3D printed hosts, including materials, processes, and geometries, needs optimization to enhance their electrochemical activity compared to anode/cathode materials. Future efforts should focus on developing photopolymerizable composite ink for efficient printing of novel 3D hosts. This will enable advancements in rechargeable battery technology, improving overall performance and energy storage capabilities.

9. Conclusion and outlook

Advanced 3DP technologies offer significant potential for practical applications in EESDs, particularly in the design and printing of 3D electrodes, flexible electrodes, and full-cells of rechargeable secondary batteries. In this report, we present the latest developments in 3DP of critical components for rechargeable secondary batteries. The use of 3DP to create various battery types (LIBs, SIBs, KIBs, ZIBs, metal batteries) with high energy and power densities represents a bold

and promising innovation, as evident from the summary and discussion of 3DP reusable batteries both domestically and internationally.

Initially, we discuss the common characteristics of primary 3DP technologies employed in constructing EESDs, focusing on design principles, material selectivity, and optimization strategies. Subsequently, we summarize recent breakthroughs in 3D-printed essential materials for rechargeable batteries, encompassing traditional Li-ion (SIBs, KIBs) batteries, Li/Na/K/Zn metal batteries, Zn-air batteries, and Ni–Fe batteries. In comparison to conventional EESDs, many thick electrodes and hierarchical porous frameworks of 3D printed electrodes demonstrate comparable or superior volumetric power density/energy densities, owing to the benefits of high mass loading of diverse active materials. Additionally, improved areal capacities, fast kinetics, as well as power and energy densities are achieved due to enhanced electrolyte wettability and accelerated ion transport, even with impressive electrode thickness and mass loadings in different battery systems. Notably, most current 3D printed electrodes are free-standing, eliminating the need for traditional current collectors (e.g., Al for cathode, Cu for anode) due to integrated manufacturing processes.

However, several barriers and challenges must be addressed to further develop 3DP technologies and promote their practical applications, despite their numerous advantages and immense potential for EESDs. Firstly, commercial 3D printers are presently limited to single-unit use and can only produce single or a few battery components, resulting in prolonged manufacturing processes. To enhance overall battery performance, it is necessary to integrate multiple functional materials rather than individual components. Therefore, decomposing the functions of 3DP equipment, improving each subsystem (molding room system, three-axis motion system, material conveying system, numerical control system), and developing integrated printing platforms are crucial.

Secondly, only a limited number of printable active materials, particularly for EESDs, are suitable as inks for rechargeable batteries. Conventional inert materials are widely used in 3DP, but to achieve optimal electrochemical performance, novel electrochemically active materials must be developed. Furthermore, inks often require various additives to fine-tune the rheology of 3D-printed electrodes, necessitating further research into multifunctional additives for 3DP rechargeable batteries.

Thirdly, nanometer-level printing precision and the development of printing technologies and equipment that can operate in low-humidity, low-oxygen environments are crucial for electrochemical energy storage and conversion systems/devices.

Fourthly, understanding the relationship between 3D designed architectures and ion transportation mechanisms is essential for improving the performance of printed batteries. Factors such as electrolyte wettability in 3D porous structures and ion transfer rates in thick electrodes can be further optimized to enhance high power densities under extreme operating conditions. Additionally, selecting the optimal manufacturing methods, process parameters, and structural parameters significantly influence the capacities and powers of batteries. Therefore, a comprehensive understanding of the interplay between electrochemical performance and structural designs is essential.

Finally, to advance commercial applications, practical production factors such as manufacturing cost, product uniformity (including structural and performance stabilities), and potential application scenarios and market sizes need to be considered. The costs of 3DP equipment and printable materials are key factors for commercial viability, and considerations such as facilities and personnel should not be overlooked. Furthermore, the safety performance of power battery products must be significantly improved to demonstrate attractive technical advantages and commercial value, particularly in high-energy density applications with reduced manufacturing costs.

Despite the challenges and drawbacks associated with developing 3D printed rechargeable batteries, we firmly believe that 3DP will become an indispensable component of future manufacturing by bridging the gap between industry and basic research through ongoing advancements in high-efficiency, low-cost, high-performance, and diverse 3DP technologies.

Acknowledgments

Y Mu, Y Chu and L Pan contributed to this work equally. This work was financially supported by Stable Support Plan Program for Higher Education Institutions (20220815094504001), and Shenzhen Key Laboratory of Advanced Energy Storage (No. ZDSYS20220401141000001).

ORCID iDs

Lyuming Pan https://orcid.org/0000-0002-6192-8385
Lin Zeng https://orcid.org/0000-0002-0510-1754

References

[1] Armand M and Tarascon J-M 2008 Building better batteries *Nature* **451** 652–7
[2] Dunn B, Kamath H K and Tarascon J-M 2011 Electrical energy storage for the grid: a battery of choices *Science* **334** 928–35
[3] Chang P, Mei H, Zhou S X, Dassios K G and Cheng L F 2019 3D printed electrochemical energy storage devices *J. Mater. Chem.* A **7** 4230–58
[4] Mackanic D G, Chang T-H, Huang Z J, Cui Y and Bao Z N 2020 Stretchable electrochemical energy storage devices *Chem. Soc. Rev.* **49** 4466–95
[5] Lv Z S, Li W L, Yang L, Loh X J and Chen X D 2019 Custom-made electrochemical energy storage devices *ACS Energy Lett.* **4** 606–14
[6] Zhao Y, Wang L, Zhou Y N, Liang Z, Tavajohi N, Li B H and Li T 2021 Solid polymer electrolytes with high conductivity and transference number of Li ions for Li-based rechargeable batteries *Adv. Sci.* **8** 2003675

[7] Liu X, Li Y, Xu X, Zhou L and Mai L 2021 Rechargeable metal (Li, Na, Mg, Al)-sulfur batteries: materials and advances *J. Energy Chem.* **61** 104–34

[8] Kim H, Choi W, Yoon J, Um J H, Lee W, Kim J, Cabana J and Yoon W-S 2020 Exploring anomalous charge storage in anode materials for next-generation Li rechargeable batteries *Chem. Rev.* **120** 6934–76

[9] Wu F X, Maier J and Yu Y 2020 Guidelines and trends for next-generation rechargeable lithium and lithium-ion batteries *Chem. Soc. Rev.* **49** 1569–614

[10] Zheng X Y, Huang L Q, Ye X L, Zhang J X, Min F Y, Luo W and Huang Y H 2021 Critical effects of electrolyte recipes for Li and Na metal batteries *Chemistry* **7** 2312–46

[11] Jin S, Jiang Y, Ji H X and Yu Y 2018 Advanced 3D current collectors for lithium-based batteries *Adv. Mater.* **30** 1802014

[12] Choi C, Ashby D S, Butts D M, DeBlock R H, Wei Q L, Lau J and Dunn B 2019 Achieving high energy density and high power density with pseudocapacitive materials *Nat. Rev. Mater.* **5** 5–19

[13] Yin F, Jin Q, Gao H, Zhang X T and Zhang Z G 2021 A strategy to achieve high loading and high energy density Li-S batteries *J. Energy Chem.* **53** 340–6

[14] Lee J, Zambrano B L, Woo J, Yoon K and Lee T 2020 Recent advances in 1D stretchable electrodes and devices for textile and wearable electronics: materials, fabrications, and applications *Adv. Mater.* **32** 1902532

[15] Fu K *et al* 2016 Graphene oxide-based electrode inks for 3D-printed lithium-ion batteries *Adv. Mater.* **28** 2587–94

[16] Pang Y K, Cao Y T, Chu Y H, Liu M H, Snyder K, MacKenzie D and Cao C Y 2020 Additive manufacturing of batteries *Adv. Funct. Mater.* **30** 1906244

[17] Yan J, Huang S Z, von Lim Y, Xu T T, Kong D Z, Li X J, Yang H Y and Wang Y 2022 Direct-ink writing 3D printed energy storage devices: from material selectivity, design and optimization strategies to diverse applications *Mater. Today* **54** 110–52

[18] Zhu C *et al* 2017 3D printed functional nanomaterials for electrochemical energy storage *Nano Today* **15** 107–20

[19] Symes M D, Kitson P J, Yan J, Richmond C J, Cooper G J T, Bowman R W, Vilbrandt T and Cronin L 2012 Integrated 3D-printed reactionware for chemical synthesis and analysis *Nat. Chem.* **4** 349–54

[20] Highley C B, Rodell C B and Burdick J A 2015 Direct 3D printing of shear-thinning hydrogels into self-healing hydrogels *Adv. Mater.* **27** 5075–9

[21] Down M P, Martínez-Periñán E, Foster C W, Lorenzo E, Smith G C and Banks C E 2019 Next-generation additive manufacturing of complete standalone sodium-ion energy storage architectures *Adv. Energy Mater.* **9** 1803019

[22] Ambrosi A and Pumera M 2016 3D-printing technologies for electrochemical applications *Chem. Soc. Rev.* **45** 2740–55

[23] Egorov V, Gulzar U, Zhang Y, Breen S and O'Dwyer C 2020 Evolution of 3D printing methods and materials for electrochemical energy storage *Adv. Mater.* **32** 2000556

[24] Tian X C, Jin J, Yuan S Q, Chua C K, Tor S B and Zhou K 2017 Emerging 3D-printed electrochemical energy storage devices: a critical review *Adv. Energy Mater.* **7** 1700127

[25] Lyu Z *et al* 2021 Design and manufacture of 3D-printed batteries *Joule* **5** 89–114

[26] Lawes S, Sun Q, Lushington A, Xiao B W, Liu Y L and Sun X L 2017 Inkjet-printed silicon as high performance anodes for Li-ion batteries *Nano Energy* **36** 313–21

[27] Lim G J H, Lyu Z Y, Zhang X, Koh J J, Zhang Y, He C B, Adams S, Wang J and Ding J 2020 Robust pure copper framework by extrusion 3D printing for advanced lithium metal anodes *J. Mater. Chem.* A **8** 9058–67

[28] Ma H, Tian X C, Wang T, Tang K, Liu Z X, Hou S E, Jin H Y and Cao G Z 2021 Tailoring pore structures of 3D printed cellular high-loading cathodes for advanced rechargeable zinc-ion batteries *Small* **17** 2100746

[29] McOwen D W *et al* 2018 3D-printing electrolytes for solid-state batteries *Adv. Mater.* **30** 1707132

[30] Sun K, Wei T-S, Ahn B Y, Seo J Y, Dillon S J and Lewis J A 2013 3D printing of interdigitated Li-ion microbattery architectures *Adv. Mater.* **25** 4539–43

[31] Zekoll S *et al* 2018 Hybrid electrolytes with 3D bicontinuous ordered ceramic and polymer microchannels for all-solid-state batteries *Energy Environ. Sci.* **11** 185–201

[32] Zhou Y H, Xia X S, Liu X P, Huang B Q, Xiao L R, Qian Q R and Chen Q H 2019 Preparation and rheological and mechanical properties of poly(butylene succinate)/talc composites for material extrusion additive manufacturing *Macromol. Mater. Eng.* **304** 1900021

[33] Zhang F, Wei M, Viswanathan V V, Swart B, Shao Y Y, Wu G and Zhou C 2017 3D printing technologies for electrochemical energy storage *Nano Energy* **40** 418–31

[34] Costa C M, Gonçalves R and Lanceros-Méndez S 2020 Recent advances and future challenges in printed batteries *Energy Storage Mater.* **28** 216–34

[35] Yu Y C, Chen M, Wang S T, Hill C, Joshi P, Kuruganti T and Hu A M 2018 Laser sintering of printed anodes for Al-air batteries *J. Electrochem. Soc.* **165** A584–92

[36] Xu Q, Lv Y Z, Dong C B, Sreeprased T S, Tian A, Zhang H Z, Tang Y, Yu Z Q and Li N 2015 Three-dimensional micro/nanoscale architectures: fabrication and applications *Nanoscale* **7** 10883–95

[37] Wei M, Zhang F, Wang W, Alexandridis P, Zhou C and Wu G 2017 3D direct writing fabrication of electrodes for electrochemical storage devices *J. Power Sources* **354** 134–47

[38] Marschewski J, Brenner L, Ebejer N, Ruch P, Michel B and Poulikakos D 2017 3D-printed fluidic networks for high-power-density heat-managing miniaturized redox flow batteries *Energy Environ. Sci.* **10** 780–7

[39] Ji D F, Zheng H Y, Zhang H, Liu W Q and Ding J W 2022 Coaxial 3D-printing constructing all-in-one fibrous lithium-, sodium-, and zinc-ion batteries *Chem. Eng. J.* **433** 133815

[40] Ao S Q, Guo Z S, Song Y C, Fang D N and Bao Y H 2022 Clog-free, low-cost, and uniform electrode inks for 3D printed lithium-ion batteries *ACS Appl. Energy Mater.* **5** 6970–9

[41] Wang J W *et al* 2018 Toward high areal energy and power density electrode for Li-ion batteries via optimized 3D printing approach *ACS Appl. Mater. Interfaces* **10** 39794–801

[42] Arenas L F, Walsh F C and de León C P 2015 3D-printing of redox flow batteries for energy storage: a rapid prototype laboratory cell *ECS J. Solid State Sci. Technol.* **4** P3080–5

[43] Maurel A, Courty M, Fleutot B, Tortajada H, Prashantha K, Armand M, Grugeon S, Panier S and Dupont L 2018 Highly loaded graphite-polylactic acid composite-based filaments for lithium-ion battery three-dimensional printing *Chem. Mater.* **30** 7484–93

[44] Zhang M G, Mei H, Chang P and Cheng L F 2020 3D printing of structured electrodes for rechargeable batteries *J. Mater. Chem.* A **8** 10670–94

[45] Acord K A, Dupuy A D, Bertoli U S, Zheng B L, West W C, Chen Q N, Shapiro A A and Schoenung J M 2021 Morphology, microstructure, and phase states in selective laser sintered lithium ion battery cathodes *J. Mater. Process. Technol.* **288** 116827

[46] Mauriello J, Maury R, Guillaneuf Y and Gigmes D 2023 3D/4D printing of polyurethanes by vat photopolymerization *Adv. Mater. Technol.* 2300366

[47] Rezaei B, Hansen T W and Keller S S 2022 Stereolithography-derived three-dimensional pyrolytic

carbon/Mn_3O_4 nanostructures for free-standing hybrid supercapacitor electrodes *ACS Appl. Nano Mater.* **5** 1808–19
[48] Hilder M, Winther-Jensen B and Clark N B 2009 Paper-based, printed zinc-air battery *J. Power Sources* **194** 1135–41
[49] Kolchanov D S, Mitrofanov I, Kim A, Koshtyal Y, Rumyantsev A, Sergeeva E, Vinogradov A, Popovich A and Maximov M Y 2020 Inkjet printing of Li-rich cathode material for thin-film lithium-ion microbatteries *Energy Technol.* **8** 1901086
[50] Zub K, Stolze C, Rohland P, Stumpf S, Hoeppener S, Hager M D and Schubert U S 2022 Inkjet-printed microband electrodes for a cost-efficient state-of-charge monitoring in redox flow batteries *Sens. Actuators* B **369** 132291
[51] Bhar M, Dey A, Ghosh S, van Spronsen M A, Selvaraj V, Kaliprasad Y, Krishnamurthy S and Martha S K 2022 Plasma jet printing induced high-capacity graphite anodes for sustainable recycling of lithium-ion batteries *Carbon* **198** 401–10
[52] Percin K, Rommerskirchen A, Sengpiel R, Gendel Y and Wessling M 2018 3D-printed conductive static mixers enable all-vanadium redox flow battery using slurry electrodes *J. Power Sources* **379** 228–33
[53] Lai C Q, Lim G Y, Tai K J, Lim K J D, Yu L H, Kanaujia P K and Seetoh P I 2022 Exceptional energy absorption characteristics and compressive resilience of functional carbon foams scalably and sustainably derived from additively manufactured kraft paper *Addit. Manuf.* **58** 102992
[54] Zhang G H, Zhang X N, Liu H Z, Li J H, Chen Y Q and Duan H G 2021 3D-printed multi-channel metal lattices enabling localized electric-field redistribution for dendrite-free aqueous Zn ion batteries *Adv. Energy Mater.* **11** 2003927
[55] Wang Z X *et al* 2022 3D-printed sodiophilic V_2CT_x/rGO-CNT MXene microgrid aerogel for stable Na metal anode with high areal capacity *ACS Nano* **16** 9105–16
[56] Wang H L, Yang Y, Liang Y Y, Cui L-F, Casalongue H S, Li Y G, Hong G S, Cui Y and Dai H J 2011 $LiMn_{1-x}Fe_xPO_4$ nanorods grown on graphene sheets for ultrahigh-rate-performance lithium-ion batteries *Angew. Chem., Int. Ed.* **50** 7364–8
[57] Airoldi L, Anselmi-Tamburini U, Vigani B, Rossi S, Mustarelli P and Quartarone E 2020 Additive manufacturing of aqueous-processed $LiMn_2O_4$ thick electrodes for high-energy-density lithium-ion batteries *Batter. Supercaps* **3** 1040–50
[58] Cao D X *et al* 2019 3D printed high-performance lithium metal microbatteries enabled by nanocellulose *Adv. Mater.* **31** 1807313
[59] Yang Y, Yuan W, Zhang X Q, Yuan Y H, Wang C, Ye Y T, Huang Y, Qiu Z Q and Tang Y 2020 Overview on the applications of three-dimensional printing for rechargeable lithium-ion batteries *Appl. Energy* **257** 114002
[60] Zhang W, Liu H Z, Zhang X N, Li X J, Zhang G H and Cao P 2021 3D printed micro-electrochemical energy storage devices: from design to integration *Adv. Funct. Mater.* **31** 2104909
[61] Zeng L, He J, Yang C Y, Luo D, Yu H B, He H N and Zhang C H 2023 Direct 3D printing of stress-released Zn powder anodes toward flexible dendrite-free Zn batteries *Energy Storage Mater.* **54** 469–77
[62] Qian J, Chen Q Y, Hong M, Xie W Q, Jing S S, Bao Y H, Chen G, Pang Z Q, Hu L B and Li T 2022 Toward stretchable batteries: 3D-printed deformable electrodes and separator enabled by nanocellulose *Mater. Today* **54** 18–26
[63] Wang Y B *et al* 2017 3D-printed all-fiber Li-ion battery toward wearable energy storage *Adv. Funct. Mater.* **27** 1703140
[64] Hensleigh R M, Cui H C, Oakdale J S, Ye J C, Campbell P G, Duoss E B, Spadaccini C M, Zheng X Y and Worsley M A 2018 Additive manufacturing of complex micro-architected graphene aerogels *Mater. Horiz.* **5** 1035–41
[65] Cheng M *et al* 2018 Elevated-temperature 3D printing of hybrid solid-state electrolyte for Li-ion batteries *Adv. Mater.* **30** 1800615
[66] Delannoy P-E, Riou B, Brousse T, Le Bideau J, Guyomard D and Lestriez B 2015 Ink-jet printed porous composite $LiFePO_4$ electrode from aqueous suspension for microbatteries *J. Power Sources* **287** 261–8
[67] Sun C, Liu S R, Shi X L, Lai C, Liang J J and Chen Y S 2020 3D printing nanocomposite gel-based thick rlectrode rnabling both high areal capacity and rate performance for lithium-ion battery *Chem. Eng. J.* **381** 122641
[68] Praveen S, Santhoshkumar P, Joe Y C, Senthil C and Lee C W 2020 3D-printed architecture of Li-ion batteries and its applications to smart wearable electronic devices *Appl. Mater. Today* **20** 100688
[69] Li K *et al* 2020 3D MXene architectures for efficient energy storage and conversion *Adv. Funct. Mater.* **30** 2000842
[70] Fan Z D, Jin J, Li C, Cai J S, Wei C H, Shao Y L, Zou G F and Sun J Y 2021 3D-printed Zn-ion hybrid capacitor enabled by universal divalent cation-gelated additive-free Ti_3C_2 MXene ink *ACS Nano* **15** 3098–107
[71] Ma J X, Zheng S H, Chi L P, Liu Y, Zhang Y, Wang K and Wu Z-S 2022 3D printing flexible sodium-ion microbatteries with ultrahigh areal capacity and robust rate capability *Adv. Mater.* **34** 2205569
[72] Fan Z D, Wei C H, Yu L H, Xia Z, Cai J S, Tian Z N, Zou G F, Dou S X and Sun J Y 2020 3D printing of porous nitrogen-doped Ti_3C_2 MXene scaffolds for high-performance sodium-ion hybrid capacitors *ACS Nano* **14** 867–76
[73] Li J, Leu M C, Panat R and Park J 2017 A hybrid three-dimensionally structured electrode for lithium-ion batteries via 3D printing *Mater. Des.* **119** 417–24
[74] Kohlmeyer R R, Blake A J, Hardin J O, Carmona E A, Carpena-Núñez J, Maruyama B, Berrigan J D, Huang H and Durstock M F 2016 Composite batteries: a simple yet universal approach to 3D printable lithium-ion battery electrodes *J. Mater. Chem.* A **4** 16856–64
[75] Ho C C, Evans J W and Wright P K 2010 Direct write dispenser printing of a zinc microbattery with an ionic liquid gel electrolyte *J. Micromech. Microeng.* **20** 104009
[76] Gao X J *et al* 2019 Toward a remarkable Li-S battery via 3D printing *Nano Energy* **56** 595–603
[77] Wu B K, Mu Y B, He J F, Li M, Li Z, Chu Y Q, Li Y J and Zeng L 2023 *In situ* characterizations for aqueous rechargeable zinc batteries *Carbon Neutralization* vol **2** pp 310–38
[78] He H N, Luo D, Zeng L, He J, Li X L, Yu H B and Zhang C H 2022 3D printing of fast kinetics reconciled ultra-thick cathodes for high areal energy density aqueous Li-Zn hybrid battery *Sci. Bull.* **67** 1253–63
[79] Pierre Mwizerwa J, Liu C Y, Xu K, Zhao N, Li Y D, Chen Z W and Shen J 2022 Three-dimensional printed lithium iron phosphate coated with magnesium oxide cathode with improved areal capacity and ultralong cycling stability for high performance lithium-ion batteries *J. Colloid Interface Sci.* **623** 168–81
[80] Xu K, Zhao N, Li Y D, Wang P, Liu Z Y, Chen Z W, Shen J and Liu C Y 2022 Design and 3D printing of interdigitated

electrode structures for high-performance full lithium-ion battery *Chin. J. Mech. Eng.* **1** 100053
[81] Hu J T *et al* 2016 3D-printed cathodes of $LiMn_{1-x}Fe_xPO_4$ nanocrystals achieve both ultrahigh rate and high capacity for advanced lithium-ion battery *Adv. Energy Mater.* **6** 1600856
[82] Ding J W, Shen K, Du Z G, Li B and Yang S B 2017 3D-printed hierarchical porous frameworks for sodium storage *ACS Appl. Mater. Interfaces* **9** 41871–7
[83] Wei T-S, Ahn B Y, Grotto J and Lewis J A 2018 3D printing of customized Li-ion batteries with thick electrodes *Adv. Mater.* **30** 1703027–34
[84] Cai J, Fan Z, Jin J, Shi Z, Dou S, Sun J and Liu Z 2020 Expediting the electrochemical kinetics of 3D-printed sulfur cathodes for Li-S batteries with high rate capability and areal capacity *Nano Energy* **75** 104970–8
[85] Lyu Z, Lim G, H J, Guo R, Kou Z, Wang T, Guan C, Ding J, Chen W and Wang J 2019 3D-printed MOF-derived hierarchically porous frameworks for practical high-energy density Li-O_2 batteries *Adv. Funct. Mater.* **29** 1806658
[86] Qiao Y, Liu Y, Chen C J, Xie H, Yao Y G, He S M, Ping W W, Liu B Y and Hu L B 2018 3D-printed graphene oxide framework with thermal shock synthesized nanoparticles for Li-CO_2 batteries *Adv. Funct. Mater.* **28** 1805899
[87] Zhang J, Li X L, Fan S, Huang S Z, Yan D, Liu L, Valdivia Y, Alvarado P and Yang H Y 2020 3D-printed functional electrodes towards Zn-air batteries *Mater. Today Energy* **16** 100407
[88] Ren Y J, Meng F B, Zhang S W, Ping B, Li H, Yin B S and Ma T Y 2022 CNT@MnO_2 composite ink toward a flexible 3D printed micro-zinc-ion battery *Carbon Energy* **4** 446–57
[89] Ahn D B, Kim W-Y, Lee K-H, Lee S-S, Kim S-H, Park S, Hong Y-K and Lee S-Y 2023 Enabling on-demand conformal Zn-ion batteries on non-developable surfaces *Adv. Funct. Mater.* **33** 2211597
[90] Liu C Y, Zhao N, Xu K, Li Y D, Mwizerwa J P, Shen J and Chen Z W 2022 High-performance $LiFePO_4$ and SiO@C/graphite interdigitated full lithium-ion battery fabricated via low temperature direct write 3D printing *Mater. Today Energy* **29** 101098
[91] Zhang C, Shen K, Li B, Li S M and Yang S B 2018 Continuously 3D printed quantum dot-based electrodes for lithium storage with ultrahigh capacities *J. Mater. Chem.* A **6** 19960–6
[92] Ragones H, Menkin S, Kamir Y, Gladkikh A, Mukra T, Kosa G and Golodnitsky D 2018 Towards smart free form-factor 3D printable batteries *Sustain. Energy Fuels* **2** 1542–9
[93] Liu C Y, Qiu Y, Liu Y L, Xu K, Zhao N, Lao C S, Shen J and Chen Z W 2022 Novel 3D grid porous $Li_4Ti_5O_{12}$ thick electrodes fabricated by 3D printing for high performance lithium-ion batteries *J. Adv. Ceram.* **11** 295–307
[94] Lyu Z Y *et al* 2020 3D-printed electrodes for lithium metal batteries with high areal capacity and high-rate capability *Energy Storage Mater.* **24** 336–42
[95] Shen K, Li B and Yang S B 2020 3D printing dendrite-free lithium anodes based on the nucleated MXene arrays *Energy Storage Mater.* **24** 670–5
[96] Foster C W, Down M P, Zhang Y, Ji X B, Rowley-Neale S J, Smith G C, Kelly P J and Banks C E 2017 3D printed graphene based energy storage devices *Sci. Rep.* **7** 42233
[97] Vasilaki E, Vernardou D, Kenanakis G, Vamvakaki M and Katsarakis N 2017 TiO_2/WO_3 photoactive bilayers in the UV-Vis light region *Appl. Phys.* A **123** 231
[98] Reyes C, Somogyi R, Niu S B, Cruz M A, Yang F C, Catenacci M J, Rhodes C P and Wiley B J 2018 Three-dimensional printing of a complete lithium ion battery with fused filament fabrication *ACS Appl. Energy Mater.* **1** 5268–79
[99] Pikul J H, Zhang H G, Cho J, Braun P V and King W P 2013 High-power lithium ion microbatteries from interdigitated three-dimensional bicontinuous nanoporous electrodes *Nat. Commun.* **4** 1732
[100] Cohen E, Menkin S, Lifshits M, Kamir Y, Gladkich A, Kosa G and Golodnitsky D 2018 Novel rechargeable 3D-microbatteries on 3D-printed-polymer substrates: feasibility study *Electrochim. Acta* **265** 690–701
[101] Chen Q M, Xu R, He Z T, Zhao K J and Pan L 2017 Printing 3D gel polymer electrolyte in lithium-ion microbattery using stereolithography *J. Electrochem. Soc.* **164** A1852–7
[102] Gu Y, Wu A D, Sohn H, Nicoletti C, Iqbal Z and Federici J F 2015 Fabrication of rechargeable lithium ion batteries using water-based inkjet printed cathodes *J. Manuf. Process.* **20** 198–205
[103] Fan Z Y, Shi J-W, Gao C, Gao G, Wang B R and Niu C M 2017 Rationally designed porous MnO_x-FeO_x nanoneedles for low-temperature selective catalytic reduction of NO_x by NH_3 *ACS Appl. Mater. Interfaces* **9** 16117–27
[104] Blake A J, Kohlmeyer R R, Hardin J O, Carmona E A, Maruyama B, Berrigan J D, Huang H and Durstock M F 2017 3D printable ceramic-polymer electrolytes for flexible high-performance Li-ion batteries with enhanced thermal stability *Adv. Energy Mater.* **7** 1602920
[105] Foroozan T, Soto F A, Yurkiv V, Sharifi-asl S, Deivanayagam R, Huang Z N, Rojaee R, Mashayek F, Balbuena P B and Shahbazian-yassar R 2018 Synergistic effect of graphene oxide for impeding the dendritic plating of Li *Adv. Funct. Mater.* **28** 1705917
[106] Lacey S D *et al* 2018 Extrusion-based 3D printing of hierarchically porous advanced battery electrodes *Adv. Mater.* **30** 1705651
[107] Zhou L, Ning W W, Wu C, Zhang D, Wei W F, Ma J M, Li C C and Chen L B 2018 3D-printed microelectrodes with a developed conductive network and hierarchical pores toward high areal capacity for microbatteries *Adv. Mater. Technol.* **4** 1800402
[108] Ma T C and MacKenzie J D 2019 Fully printed, high energy density flexible zinc-air batteries based on solid polymer electrolytes and a hierarchical catalyst current collector *Flex. Print. Electron.* **4** 015010
[109] Brown E, Yan P L, Tekik H, Elangovan A, Wang J, Lin D and Li J 2019 3D printing of hybrid MoS_2-graphene aerogels as highly porous electrode materials for sodium ion battery anodes *Mater. Des.* **170** 107689
[110] Zhao Y M, Zhou Q, Liu L, Xu J, Yan M M and Jiang Z Y 2006 A novel and facile route of ink-jet printing to thin film SnO_2 anode for rechargeable lithium ion batteries *Electrochim. Acta* **51** 2639–45
[111] Silverwood I P, Rogers S M, Callear S K, Parker S F and Catlow C R A 2016 Evidence for a surface gold hydride on a nanostructured gold catalyst *Chem. Commun.* **52** 533–6
[112] Ho C C, Murata K, Steingart D A, Evans J W and Wright P K 2009 A super ink jet printed zinc-silver 3D microbattery *J. Micromech. Microeng.* **19** 094013
[113] Budai J D, Liu W, Tischler J Z, Pan Z W, Norton D P, Larson B C, Yang W and Ice G E 2008 Polychromatic x-ray micro- and nanodiffraction for spatially-resolved structural studies *Thin Solid Films* **516** 8013–21
[114] Xia Y Q, Tang Y, Yu X, Wan Y, Chen Y Z, Lu H G and Zheng S-Y 2017 Label-free virus capture and release by a microfluidic device integrated with porous silicon nanowire forest *Small* **13** 1603135
[115] Mauger A, Armand M, Julien C M and Zaghib K 2017 Challenges and issues facing lithium metal for solid-state rechargeable batteries *J. Power Sources* **353** 333–42

[116] Li N-W, Shi Y, Yin Y-X, Zeng X-X, Li J-Y, Li C-J, Wan L-J, Wen R and Guo Y-G 2018 A flexible solid electrolyte interphase layer for long-life lithium metal anodes *Angew. Chem., Int. Ed.* **57** 1505–9

[117] Xu R, Zhang X-Q, Cheng X-B, Peng H-J, Zhao C-Z, Yan C and Huang J-Q 2018 Artificial soft-rigid protective layer for dendrite-free lithium metal anode *Adv. Funct. Mater.* **28** 1705838

[118] Idrees M, Batool S, Cao J W, Javed M S, Xiong S F, Liu C Y and Chen Z W 2022 3D printed PC/SiOC@Zn hybrid composite as dendrite-free anode for Zn-ion battery *Nano Energy* **100** 107505

[119] Wu B K, Guo B B, Chen Y Z, Mu Y B, Qu H Q, Lin M, Bai J M, Zhao T S and Zeng L 2023 High zinc utilization aqueous zinc ion batteries enabled by 3D printed graphene arrays *Energy Storage Mater.* **54** 75–84

[120] Yan J *et al* 2020 3D printed rGO/CNT microlattice aerogel for a dendrite-free sodium metal anode *J. Mater. Chem.* A **8** 19843–54

[121] Luo W, Lin C-F, Zhao O, Noked M, Zhang Y, Rubloff G W and Hu L B 2017 Ultrathin surface coating enables the stable sodium metal anode *Adv. Energy Mater.* **7** 1601526

[122] Shi H T, Pei M F, Wang S, Yao F T, Xia Y H, Xu Z W, Liu S K, Shao R Q, Wang W and Liang S T 2023 3D-printed periodic hierarchical porous rGO/$Ti_3C_2T_x$ architectures induced uniform lithium deposition for Li metal anodes *Adv. Mater. Technol.* **8** 2200256

[123] Sun C W, Liu J, Gong Y D, Wilkinson D P and Zhang J J 2017 Recent advances in all-solid-state rechargeable lithium batteries *Nano Energy* **33** 363–86

[124] Zhang C Y, Wang A X, Zhang J H, Guan X Z, Tang W J and Luo J Y 2018 2D materials for lithium/sodium metal anodes *Adv. Energy Mater.* **8** 1802833

[125] Vlad A, Singh N, Galande C and Ajayan P M 2015 Design considerations for unconventional electrochemical energy storage architectures *Adv. Energy Mater.* **5** 1402115

[126] Cao J, Zhang D D, Chanajaree R, Yue Y L, Zeng Z Y, Zhang X Y and Qin J Q 2022 Stabilizing zinc anode via a chelation and desolvation electrolyte additive *Adv. Powder Mater.* **1** 100007

[127] Fang G Z, Zhou J, Pan A Q and Liang S Q 2018 Recent advances in aqueous zinc-ion batteries *ACS Energy Lett.* **3** 2480–501

[128] Guo S, Qin L P, Zhang T S, Zhou M, Zhou J, Fang G Z and Liang S Q 2021 Fundamentals and perspectives of electrolyte additives for aqueous zinc-ion batteries *Energy Storage Mater.* **34** 545–62

[129] Yang Q *et al* 2020 Hydrogen-substituted graphdiyne ion tunnels directing concentration redistribution for commercial-grade dendrite-free zinc anodes *Adv. Mater.* **32** 2001755

[130] Ma H, Tian X C, Fan J T, Cao W Y, Yuan X L, Hou S E and Jin H Y 2022 3D printing of solid-state zinc-ion microbatteries with ultrahigh capacity and high reversibility for wearable integration design *J. Power Sources* **550** 232152

[131] Liu H *et al* 2020 Controlling dendrite growth in solid-state electrolytes *ACS Energy Lett.* **5** 833–43

[132] Liu Z X *et al* 2021 Direct ink writing of $Li_{1.3}Al_{0.3}Ti_{1.7}PO_4{}^3$-based solid-state electrolytes with customized shapes and remarkable electrochemical behaviors *Small* **17** 2002866

[133] Pang Q, Liang X, Shyamsunder A and Nazar L F 2017 An *in vivo* formed solid electrolyte surface layer enables stable plating of Li metal *Joule* **1** 871–86

[134] Sun N *et al* 2019 Anisotropically electrochemical-mechanical evolution in solid-state batteries and interfacial tailored strategy *Angew. Chem., Int. Ed.* **58** 18647–53

[135] Yang Q, Liang G J, Guo Y, Liu Z X, Yan B X, Wang D H, Huang Z D, Li X L, Fan J and Zhi C Y 2019 Do zinc dendrites exist in neutral zinc batteries: a developed electrohealing strategy to *in situ* rescue in-service batteries *Adv. Mater.* **31** 1903778

[136] Yang H Y *et al* 2022 A simple and effective host for sodium metal anode: a 3D-printed high pyrrolic-N doped graphene microlattice aerogel *J. Mater. Chem.* A **10** 16842–52

[137] He Y J, Chen S J, Nie L, Sun Z T, Wu X S and Liu W 2020 Stereolithography three-dimensional printing solid polymer electrolytes for all-solid-state lithium metal batteries *Nano Lett.* **20** 7136–43

[138] Ling W, Fu N, Yue J P, Zeng X-X, Ma Q, Deng Q, Xiao Y, Wan L-J, Guo Y-G and Wu X-W 2020 A flexible solid electrolyte with multilayer structure for sodium metal batteries *Adv. Energy Mater.* **10** 1903966

[139] Zeng L, He H N, Chen H Y, Luo D, He J and Zhang C H 2022 3D printing architecting reservoir-integrated anode for dendrite-free, safe, and durable Zn batteries *Adv. Energy Mater.* **12** 2103708

[140] Mangani L R and Villevieille C 2020 Mechanical vs. chemical stability of sulphide-based solid-state batteries. Which one is the biggest challenge to tackle? Overview of solid-state batteries and hybrid solid state batteries *J. Mater. Chem.* A **8** 10150–67

[141] Tian X C and Xu B G 2021 3D printing for solid-state energy storage *Small Methods* **5** 2100877

[142] Stephen A, Bhoyate S, Cao P F, Advincula R, Dahotre N, Jiang Y J and Choi W 2022 3D-printed flexible anode for high-performance zinc ion battery *MRS Commun.* **12** 894–901

[143] Cheng M and Jiang Y 2021 3D-printed solid-state electrolytes for electrochemical energy storage devices *J. Mater. Res.* **36** 4547–64

[144] Deiner L J, Bezerra C A G, Howell T G and Powell A S 2019 Digital printing of solid-state lithium-ion batteries *Adv. Eng. Mater.* **21** 1900737

[145] Fan L L and Li X F 2018 Recent advances in effective protection of sodium metal anode *Nano Energy* **53** 630–42

[146] Nagaraju G, Tagliaferri S, Panagiotopoulos A, Och M, Quintin-Baxendale R and Mattevi C 2022 Durable Zn-ion hybrid capacitors using 3D printed carbon composites *J. Mater. Chem.* A **10** 15665–76

[147] Lu Y Y, Tu Z Y and Archer L A 2014 Stable lithium electrodeposition in liquid and nanoporous solid electrolytes *Nat. Mater.* **13** 961–9

[148] Liu Y, Qiao Y, Zhang Y, Yang Z, Gao T T, Kirsch D, Liu B Y, Song J W, Yang B and Hu L B 2018 3D printed separator for the thermal management of high-performance Li metal anodes *Energy Storage Mater.* **12** 197–203

[149] Wang L G, Li J, Lu G L, Li W Y, Tao Q Q, Shi C H, Jin H L, Chen G and Wang S 2020 Fundamentals of electrolytes for solid-state batteries: challenges and perspectives *Front. Mater.* **7** 111

[150] Liu P G, Zhang Z Y, Hao R, Huang Y P, Liu W F, Tan Y Y, Li P L, Yan J and Liu K Y 2021 Ultra-highly stable zinc metal anode via 3D-printed g-C_3N_4 modulating interface for long life energy storage systems *Chem. Eng. J.* **403** 126425

[151] Lin D C, Liu Y Y, Liang Z, Lee H-W, Sun J, Wang H T, Yan K, Xie J and Cui Y 2016 Layered reduced graphene oxide with nanoscale interlayer gaps as a stable host for lithium metal anodes *Nat. Nanotechnol.* **11** 626–32

[152] Ragones H, Vinegrad A, Ardel G, Goor M, Kamir Y, Dorfman M M, Gladkikh A and Golodnitsky D 2020 On the road to a multi-coaxial-cable battery: development of a novel 3D-printed composite solid electrolyte *J. Electrochem. Soc.* **167** 070503

[153] Maurel A, Armand M, Grugeon S, Fleutot B, Davoisne C, Tortajada H, Courty M, Panier S and Dupont L 2020 Poly(ethylene oxide)-LiTFSI solid polymer electrolyte filaments for fused deposition modeling three-dimensional printing *J. Electrochem. Soc.* **167** 070536
[154] Liu Y, Zheng S H, Ma J X, Wang X, Zhang L Z, Das P, Wang K and Wu Z-S 2022 All 3D printing shape-conformable zinc ion hybrid capacitors with ultrahigh areal capacitance and improved cycle life *Adv. Energy Mater.* **12** 2200341
[155] Li W Y, Yao H B, Yan K, Zheng G Y, Liang Z, Chiang Y-M and Cui Y 2015 The synergetic effect of lithium polysulfide and lithium nitrate to prevent lithium dendrite growth *Nat. Commun.* **6** 7436
[156] Qi G A, Zeng Y and Chen J M 2022 Preparation of porous SnO_2-based ceramics with lattice structure by DLP *Ceram. Int.* **48** 14568–77
[157] Wang S, Shi H T, Xia Y H, Liu D, Min C Y, Zeng M, Liang S R, Shao R Q, Wu X Q and Xu Z W 2022 A 3D-printed framework with a gradient distributed heterojunction and fast Li^+ conductivity interfaces for high-rate lithium metal anodes *J. Mater. Chem.* A **10** 24258–68
[158] Shen K, Cao Z J, Shi Y Z, Zhang Y Z, Li B and Yang S B 2021 3D printing lithium salt towards dendrite-free lithium anodes *Energy Storage Mater.* **35** 108–13
[159] Chen T, Wang Y N, Yang Y, Huang F, Zhu M K, Ang B T W and Xue J M 2021 Heterometallic seed-mediated zinc deposition on inkjet printed silver nanoparticles toward foldable and heat-resistant zinc batteries *Adv. Funct. Mater.* **31** 2101607
[160] Zhou S, Usman I, Wang Y J and Pan A Q 2021 3D printing for rechargeable lithium metal batteries *Energy Storage Mater.* **38** 141–56
[161] Zhang Y *et al* 2017 High-capacity, low-tortuosity, and channel-guided lithium metal anode *Proc. Natl Acad. Sci. USA* **114** 3584–9
[162] Wang C H, Kim J T, Wang C S and Sun X L 2023 Progress and prospects of inorganic solid-state electrolyte-based all-solid-state pouch cells *Adv. Mater.* **35** 2209074
[163] Harry K J, Hallinan D T, Parkinson D Y, MacDowell A A and Balsara N P 2014 Detection of subsurface structures underneath dendrites formed on cycled lithium metal electrodes *Nat. Mater.* **13** 69–73
[164] He P and Huang J X 2021 Detrimental effects of surface imperfections and unpolished edges on the cycling stability of a zinc foil anode *ACS Energy Lett.* **6** 1990–5
[165] Blachowicz T and Ehrmann A 2020 3D printed MEMS technology-recent developments and applications *Micromachines* **11** 434
[166] Ning H L, Pikul J H, Zhang R Y, Li X J, Xu S, Wang J J, Rogers J A, King W P and Braun P V 2015 Holographic patterning of high-performance on-chip 3D lithium-ion microbatteries *Proc. Natl Acad. Sci. USA* **112** 6573–8